DESIGNING A MODELING FRAMEWORK FOR ESTIMATING SOIL MOISTURE IN HETEROGENOUS LANDSCAPE

A Thesis

by

SAMAGRA RANA

Submitted to the Office of Graduate and Professional Studies of
Texas A&M University
in partial fulfillment of the requirements for the degree of

MASTER OF SCIENCE

Chair of Committee,	Binayak Mohanty
Committee Members,	Anthony Cahill
	Patricia Smith
Head of Department,	Stephen Searcy

May 2016

Major Subject: Biological and Agricultural Engineering

ABSTRACT

Soil moisture is an important component in many hydrologic and land–atmosphere interactions. Proper characterization of soil moisture variability is vital for understanding hydrological, ecological and biogeochemical processes. At the Darcy scale, root zone soil moisture variability can effectively be estimated by employing an accurate process based model. In this study, we used different conceptual soil-water flow models (single porosity and dual porosity) to predict soil moisture variability across the Little Washita watershed, Oklahoma. The soil hydraulic parameters (SHPs) for the models were estimated through inverse modeling of multi-step outflow experimental data from soil cores, collected during the Southern Great Plains (SGP) 1997 hydrology experiment, from various parts of the watershed. Single porosity, bimodal and dual porosity models were used to calculate SHPs. With the application of various soil water flow model, non-equilibrium effects and preferential flow were briefly discussed. The validity of different models is presented based on the landscape position (location) characteristics (soil, topography, vegetation, organic matter content) of the soil cores. Using calculated SHPs from various parts of the watershed, soil moisture was predicted using forward modeling from March 1997 to November 1997. Different combinations of soil texture, topography, vegetation and organic content influenced the soil hydraulic properties and in soil moisture prediction. For most of the soil samples, dual porosity model was able to capture the micro and macro heterogeneities better than Durner's and single porosity model. But factors such as landscape position, organic matter and

vegetation significantly contributed in predicting soil moisture. Our soil moisture predictions were validated with remotely sensed soil moisture values. Based on our validation, a combination modeling scheme is suggested for soil water model selection for various parts of the watershed.

DEDICATION

To my dear parents and my loving wife, Ritika, for their patience and encouragement.

ACKNOWLEDGEMENTS

The realization of this dissertation would not have been possible without the help and support of several people. I owe this gratitude to my family, advisors, teachers and friends who have truly enhanced my graduate experience.

I would like to acknowledge my committee chair Dr. Binayak Mohanty for his passionate guidance, constant encouragement and invaluable advice. I cannot thank him enough for the data provided by him for this study. I have been fortunate to have an advisor who gave me the liberty to explore ideas and work on them. I also wish to thank Dr. Antony Cahill and Dr. Patricia Smith who freely shared their time with me and for their guidance and insight throughout the course of this research. I sincerely want to thank Dr. Binayak Mohanty, Map & GIS Libraries, Engineering Academic and Student Affairs (EASA) and the Department of Biological and Agricultural Engineering for supporting my graduate studies financially.

I would like to take this opportunity to sincerely thank my colleague Dr. Nandita Gaur for providing valuable suggestions and constructive feedback that helped me immensely in my research work. My special thanks to Mr. Zhenglei Yang, for his valuable inputs and advise in the beginning phase of my graduate program. I also acknowledge invaluable support from my other colleagues, Jonggun, Neelam and Dhruva.

I would like to extend my thanks to all of my friends for their unselfish assistance, suggestions and great company which made my stay at College Station a

great one. Gratitude also goes to the department faculty and staff for making my time at Texas A&M University a great experience.

Finally, thanks to my parents for their encouragement and to my wife for her patience and love.

NOMENCLATURE

AIC	Akaike Information Criterion
BIC	Bayes Information Criterion
DNE	Dynamic Non Equilibrium
DOY	Day of Year
DPM	Dual Porosity Model
ESTAR	Electronically Scanned Thinned Array Radiometer
HCF	Hydraulic Conductivity Function
MAE	Mean Absolute Error
MSO	Multistep Outflow Experiment
PDF	Probability Density Function
REV	Representative Elementary Volume
RMSE	Root Mean Square Error
SGP97	Southern Great Plains 1997
SHP	Soil Hydraulic Properties
SPM	Single Porosity Model
TS	Time Stable
VGM	Van Genuchten Model
WRC	Water Retention Curve

TABLE OF CONTENTS

Page

LIST OF FIGURES

Page

LIST OF TABLES

Page

CHAPTER I

INTRODUCTION

1.1 Background

The water flow in the vadose zone is studied and predicted with the help of soil hydraulic properties (SHPs) which play a key role in environmental sciences. SHPs are vital to describe not only water flow but also help in predicting transport and fate of contaminants in the vadose zone [*Hanson et al.,* 1999]. They not only help to predict water content in the porous media at various scales but also impact water and energy fluxes like evaporation from soil and transpiration from plants. Therefore, SHPs are vital to improve our understanding of the water and energy budget.

One of the most important components of the water budget is the amount of water content present in soil at multiple scales. Specifically, soil moisture plays a very important role in regulating various processes of the hydrological cycle. It affects the partitioning of precipitation into infiltration and runoff, thereby regulating the extent of groundwater recharge and the fate and transport of contaminants on the surface and sub-surface. Soil moisture also contributes in the root zone, for growth and development of plants. But it has been observed that soil moisture distribution across the land surface and in the vadose zone is highly variable. Soil moisture at any location is the net result of antecedent conditions, environmental factors, and the local physical characteristics of the soil [*Castillo et al.,* 2003]. It is well known that even homogenous soil is composed of a distribution of soil particles and pore sizes that cause variations in physical properties over small distances [*Messing and Jarvis,* 1990; *Jarvis,* 2007]. These

variations may occur at micro scales or at larger scales. At micro scales, these variations are observed in physical properties and lead to preferential flow and other such processes at continuum scale. At macro scales, soil moisture variation may be classified according to the scale of variation of the physical factors causing the soil moisture to vary. For instance, factors such as soil texture, land cover, soil depth, topography and organic matter content often cause the soil moisture to vary at the same spatial scale [*Gaur and Mohanty*, 2013]. All these factors are expected to have some influence on soil moisture but the effects may not always be similar.

1.2 Motivation

Soil hydraulic properties are estimated by various techniques at different scales like laboratory or in-situ measurement, numerical modeling using in-situ soil moisture and soil matric potential observations and data assimilation using remote sensing soil moisture. Soil water flow is dependent on soil structure which in field conditions can depend on soil type (texture), landscape position, vegetation and organic matter content. However, models developed for soil water flow are typically designed using laboratory experiments for different soil types. These models do not account for field conditions like differences in topographic positions, vegetation cover, etc., which can alter soil structure and thus water flow. This leads to the uncertainties associated with prediction of SHPs magnified at various scales. Thus the motivation for this study is to assess the efficacy of different model parameterization of the soil water characteristic curve and soil hydraulic conductivity curve under field conditions at different landscape positions. This motive led to this research, in which we examined how soil moisture variability and

its distribution are dependent on soil hydraulic properties and also determined the major physical factors contributing to this variability in different parts of the study watershed. We measured soil moisture at a number of points within the study watershed and derived a reference map from the measured values. Design of the necessary sampling network will be easier if the relationships between the physical factors causing the soil moisture to vary and the accuracy of the resulting soil moisture can be established.

1.3 Research Objectives

The overarching objective of this research was to illustrate the spatial variability in water flow and root zone soil moisture distribution at various landscape positions through SHP measurement and numerical modeling.

The specific objectives of this research include:

- To quantify the appropriate parameterization of soil hydraulic properties under non-equilibrium conditions.
- To predict the spatio-temporal variability of soil moisture across the Little Washita watershed in Oklahoma using land-surface heterogeneity specific soil water flow models.

In Chapter II, different soil water flow models were used for parameterization of soil hydraulic properties of soil samples collected from different landscape positions. These soil samples varying in terms of soil texture, soil depth, topography, vegetation and organic matter were collected from various locations within the Little Washita watershed, Oklahoma. These samples were used to estimate SHPs using inverse modeling with dynamic and static data using a multistep experiment in the laboratory.

Various approaches for modeling (single and dual porosity continuum scale models) preferential and non-equilibrium flow in the vadose zone were reviewed. Difference in soil water flow movement under similar conditions was observed and probable causes were discussed based on dynamic outflow observations at a continuum scale. We also observed that field scale factors such as soil texture, topography and vegetation cover variably affected the soil water flow.

We used the estimated SHPs to predict soil moisture over a period of time (crop growing and dormant seasons) using forward modeling with attention to the landscape position encompassing similar soil texture, topography, vegetation and organic matter using the single and dual porosity models. We observed that the highly non-linear soil moisture distribution across depth and its spatial variability was dependent on landscape positions within the watershed. The predicted soil moisture values at time stable locations were validated with remote sensing observations. In summary, a modeling scheme was developed to help the user select the best continuum-scale soil water flow model to characterize soil hydraulic properties based on different landscape positions (with various texture, topography, vegetation).

CHAPTER II

PARAMETERIZATION OF SHPS AND SOIL MOISTURE PREDICTION

2.1 Literature Review

Knowledge of spatially distributed soil hydraulic parameters (SHPs) is necessary to study and solve many problems related to agriculture, ecology, water management and flood and drought prediction [*Diamantopoulos and Durner,* 2012; *Mohanty and Zhu,* 2007; *Šimůnek,* 2005]. Soil hydraulic properties define the relationships between soil matrix potential (or capillary head), h, and the soil water content, θ (expressed volumetrically or gravimetrically). SHPs are often described as a water retention curve (WRC) and the hydraulic conductivity function (HCF) [*Assouline and Or,* 2013; *Durner et al.,* 1999b]. To determine the SHPs, the conventional laboratory measurements of saturated hydraulic conductivity, K_s, and HCF is very time consuming, tedious and expensive [*Hopmans et al.,* 2002; *Nasta et al.,* 2009; *Tuli et al.,* 2001].

Within the last two decades, parameterization of SHPs by inverse modeling from transient outflow measurement [*Eching and Hopmans,* 1993; *Eching et al.,* 1994; *Tuli et al.,* 2001] has been widely accepted. In literature, inflow/outflow experiments have provided sufficient information to uniquely identify the parameters of retention and the unsaturated conductivity function [*Durner et al.,* 1999c; *Klute and Dirksen,* 1986]. Modeling of water flow at continuum scale has been described by single porosity models, such as *van Genuchten* [1980] and *Ross and Smetten* [2000]. In the past two decades researchers have realized the importance of mobile-immobile models and dual permeability models [*Šimůnek et al.,* 2003]. Although these models are complex, they

have successfully improved predictions describing preferential flow at continuum scale. Preferential flow as opposed to uniform flow, results in irregular wetting of the soil profile as a direct consequence of water moving faster in certain parts of the soil profile than in others [*Jarvis,* 2007]. The water content front can spread quickly to greater depths while bypassing a large part of the matrix pore space [*Flühler et al.,* 1996; *Skopp,* 1981]. At times, the movement of water may move further to greater depths, and much faster than would be predicted by Richard's equation [*Beven,* 1991]. *Jarvis* [1998] considered non-equilibrium to be the most important feature of preferential flow by defining it as a flow regime in which 'for various reasons, infiltrating water does not have sufficient time to equilibrate with slowly moving resident water in the bulk of the soil matrix'.

Previous studies have described non-equilibrium water flow in the vadose zone [*Diamantopoulos et al.,* 2012; *Köhne et al.,* 2009; *Nielsen et al.,* 1986; *Šimůnek and van Genuchten,* 2008]. These studies also discuss various physical processes at continuum scale and also include water flow models in vadose zone. Porous media often exhibits a variety of heterogeneities, such as fractures, fissures, cracks and macropores which affect the water movement. The comparison of equilibrium and non-equilibrium models describes variable flow mechanisms and processes by describing macropore heterogeneity at continuum scale. Unsaturated water flow models such as, *van Genuchten* [1980], Durner's [1994] and concepts of dual porosity or permeability models [*Philip,* 1968; *Gerke and Genuchten,* 1993] have successfully shown how heterogeneity of soil described water flow paths differently at continuum scale under

laboratory conditions. However, the same does not hold true for field and watershed scale. Many other underlying heterogeneity factors such as soil type, topography, precipitation gradient, organic matter, vegetation and soil depth [*Gaur and Mohanty,* 2013] play an equally important role in water flow in the unsaturated zone. We want to explore these uncertainties at field scale and assess the applicability of continuum scale water flow models under field conditions. Ideally, van Genuchten-Mualem model (VGM) would be sufficient to describe water flow in homogenous porous system as it is described for soil as a single porosity system e.g., sand. In Durner's model, a multimodal retention function is described and is dependent on the pore size distribution in the overlapping porous soil system. Durner's model should be able to indicate hydraulic conductivity function more effectively than a unimodal conductivity function (VGM), since most porous systems are heterogeneous e.g. loamy sand or silty loam. Similarly, Dual Porosity Model (DPM) is assumed that the porous medium consists of two interacting regions, one associated with the inter-aggregate, macropore or fracture system and one comprising micropores (or intra-aggregate pores) inside soil aggregates or the matrix. Clayey types of soils are a good example of this type of porous system.

At the pore scale, non-equilibrium effects are observed in water flow because of various reasons, such as fluid-fluid interface dynamics [*Hassanizadeh et al.,* 2002], entrapment of water or pore water blockage [*Wildenschild et al.,* 2001], air entrapment [*Schultze et al.,* 1997], dynamic contact angle [*Friedman,* 1999], microheterogenity [*Mirzaei and Das,* 2007] and large scale heterogeneity [*Vogel et al.,* 2010]. Under field conditions, factors such as organic matter content and vegetation (roots) alter the soil

porosity. Also, topography tends to influence factors such as vegetation density, soil depth and erodibility, thereby altering the soil water retention and flow characteristics. Overall, soil systems, (and their SHPs) are influenced by many factors, including soil texture, structure, organic matter content, plant roots, topography, soil micro-organisms and management practices [*Shin et al.*, 2012].

In this study, using soil water retention and multi-step dynamic outflow data, soil hydraulic properties were calculated and compared for various water flow models by inverse modeling. The calculated soil hydraulic properties are classified and segregated based on soil type, topography, organic matter and soil depth across the study watershed. Using these SHPs, soil moisture are calculated across the watershed using a forward modeling scheme. The predicted soil moisture was validated using time stable remotely sensed soil moisture at time stable locations [*Joshi et al*., 2011]. A simple scheme for selecting continuum scale unsaturated water flow models based on landscape position and other physical features is proposed.

2.1.1 Time Stable Locations

As science is becoming more and more dependent on remotely derived hydrological parameters such as soil moisture, remote sensing of soil moisture measurements needs to be calibrated and validated using soil moisture measurements on ground [*Yoo,* 2002]. This calibration and validation of remotely sensed soil moisture is done with soil moisture obtained from ground sampling. Remote sensing validation necessitates having specific locations within a field that can estimate mean soil moisture over a long period of time. These locations are called time stable (TS) locations

[*Vachaud et al.,* 1985; *Mohanty and Skaggs,* 2001]. The time stability concept was introduced by *Vachaud et al*. [1985] and has been widely used to analyze the time stable characteristics of soil moisture fields and determine the TS locations which are the representative of the field. With the help of these locations, effective representative soil moisture values can be calculated and prove useful in designing hydrology experiments and remote sensing validations [*Mohanty and Skaggs,* 2001]. TS locations can help in determine physical controls affecting the soil moisture spatiotemporal variability at different scales [*Mohanty et al.,* 2000; *Jacobs et al.,* 2004]. Theoretically, time stability is the time-invariant association between spatial location and classical statistical parametric values of different soil properties. *Mohanty and Skaggs* [2001] studied the effects of soil type, slope and vegetation on the spatiotemporal evolution and time stability of soil moisture. Their study was focused in three fields in the Southern Great Plains region and used theta probes and remote sensing data. Significantly, they found that the sandy loam field exhibited better TS features compared to the other two fields containing silt loam soils. They also observed that the field having flat topography had the worst time stability compared to the two fields with gently rolling topography. *Joshi et al.* [2011] examined the TS characteristics of remotely sensed footprints at the Little Washita watershed in Oklahoma. Specifically, they compared the footprint-scale TS features with ground based soil moisture analyses to determine the common physical controls affecting the spatio-temporal evolution of soil moisture at different measurement scales. They also determined specific TS locations in the Little Washita watershed and found that the fields having rolling topography were slightly more stable

than flat topography. Overall, they found that field sites with sandy loam and loam soil texture were best indicators for time stability phenomena. In terms of hillslope, footprints with mild slope were best suited for time stability whereas vegetation and land cover did not influence soil moisture time stability.

2.2 Conceptual and Physical Models

The physical principles that govern flow and capillary processes in the vadose zone at the local scale is well established and is described by Richard's equation.

$$C(h)\frac{\partial h}{\partial t} = \frac{\partial}{\partial z}\left[K(h)\frac{\partial h}{\partial z}\right] - \frac{\partial K(h)}{\partial z} + S \qquad (2.1)$$

where θ [L^3 L^{-3}] is the volumetric water content; $C(h)=\delta\theta/\delta h$ is the soil water capacity;t [T] is the time; while S represents sources or sinks of water in the system. $K(h)$ is the unsaturated hydraulic conductivity function and the saturated hydraulic conductivity, often given as a product of the relative hydraulic conductivity, K_r (dimensionless) and the saturated hydraulic conductivity Ks [LT^{-1}]. Richard's equation is assumed to be valid if the porous system is rigid, non-swelling, isotropic and only if isothermal liquid (water) flow takes place. It is also assumed that air is free to move without notable pressure variations in the soil at any system state. Many unsaturated water flow numerical models (e.g. HYDRUS 1D (*Simunek et al*., 2008), SWAP (*van Dam et al*. 1997) etc.) are usually based on Richard's equation.

Several models have been used to describe characteristic features of preferential flow and sources of non-equilibrium. For physical non equilibrium processes, a common approach has been the use of continuum scale models such as single porosity, dual

porosity and dual permeability models [*Feyen et al.,* 1998; *Gee et al.,* 1991; *Šimůnek et al.,* 2003]. In this study we consider van Genuchten [1980], Durner [1994] and dual porosity model (DPM). With these three models, preferential water flow in structured media may be predicted differently [*Gerke and Genuchten,* 1993; *Jarvis,* 1998] based on the complexity of the soil system. Each model is developed with different conceptual framework based on pore size distribution and their functionality at a continuum or representative elementary volume (REV) scale. Other factors such as soil texture, structure, organic matter, vegetation/roots, and topographic position become relevant when water flow is predicted under field conditions. We evaluated the performance of the various soil hydraulic models under different physical factors at larger scale.

2.2.1 van Genuchten Model

Single porosity model (SPM) is the most basic approach to describe water flow through a single domain representation (Figure 1a). One of the most popular relationship used to calculate SHPs is *van Genuchten* [1980] and *Mualem* [1976]

$$\theta(h) = \begin{cases} \theta_r + \dfrac{\theta_s - \theta_r}{\left[1 + |\alpha h|^n\right]^m} & h < 0 \\ \theta_s & h > 0 \end{cases} \qquad (2.2)$$

$$K(h) = K_s K_e^{\,l} \left[1 - (1 - S_e^{1/m})^m\right]^2 \qquad (2.3)$$

where θ_r and θ_s denotes the residual and saturated water contents ($L^3\ L^{-3}$), respectively; K_s ($L\ T^{-1}$) is the saturated hydraulic conductivity, α(L^{-1}) and *n* are empirical coefficients

affecting the shape of the hydraulic functions, l is a pore connectivity parameter, m=1−1/n, and S_e is effective saturation:

$$S_e(h) = \frac{\theta(h) - \theta_r}{\theta_s - \theta_r} \tag{2.4}$$

2.2.2 Durner's Model

Multimodal retention functions can be defined if the soil is composed of more than one pore size distribution system. A very simplistic approach of dual porosity was taken by *Durner* [1994]. In this study, he combined Richard's equation with double hump type composite functions for calculating SHPs, as shown in Figure 1b. This linear superposition of the functions for each particular region gives the functions for the entire multi-modal pore system [*Durner et al.,* 1999a].

$$S_e(h) = \frac{\theta(h) - \theta_r}{\theta_s - \theta_r} = \sum_{i=1}^{k} w_i \frac{1}{(1 + (\alpha_i h)^{n_1})^{m_1}} \tag{2.5}$$

$$K(\theta) = K_s \left(\sum_{i=1}^{k} w_i S_{e_i} \right)^{l} \frac{\left(\sum_{i=1}^{k} w_i \alpha_i \left[1 - \left(1 - S_{e_i}^{1/m_i} \right)^{m_i} \right] \right)^2}{\left(\sum_{i=1}^{k} w_i \alpha_i \right)} \tag{2.6}$$

where S_e is the effective water content, and θ_r, and θ_s denote the residual and saturated water contents, respectively. The integer k denotes the number of overlapping sub-regions, w_i are the weighting factors for the sub-curves and α_i, n_i, $m_i=(1-1/n_i)$, and l are empirical parameters of the sub-curves. The hydraulic characteristics defined by Eqs. *2.5* and *2.6* which contain 4+2k unknown parameters. In these functions, θ_r, θ_s, and K_s have

a physical meaning, whereas α_i, n_i and l are essentially empirical parameters determining the shape of the retention and hydraulic conductivity functions.

2.2.3 Dual Porosity Model

In dual porosity models [*Philip,* 1968; *Van Genuchten and Wierenga,* 1976] it is assumed that water flow occurs only through the fractures (or inter-aggregate pores and macropores) and that water in the matrix (intra-aggregate pores or the matrix) is immobile. The schematic representation of this model is shown in Figure 1c. In this conceptualization the two regions are distinguished as mobile (region which allows water flow, θ_f) and immobile (region in which the pores in the matrix can exchange, retain and store water, θ_m but does not permit convective flow). We have used '*f*' to represent fractures (inter-aggregate pores) and '*m*' to represent matrix (intra-aggregate pores or rock matrix) in subscripts for respective soil representation. The total water comprises of the water present in mobile and immobile phase

$$\theta = \theta_f + \theta_m \tag{2.7}$$

with some exchange of water between the two regions which is calculated by means of a first order process. This model is formulated as a combination of modified Richards' equation which describes water flow in fractures and a mass balance equation to describe moisture dynamics in the matrix as

$$\frac{\partial \theta_f}{\partial t} = \frac{\partial}{\partial t}\left[K(h)\left(\frac{\partial h}{\partial z} + 1 \right) \right] - S_f - \Gamma_w \tag{2.8}$$

$$\frac{\partial \theta_m}{\partial t} = -S_m + \Gamma_w \tag{2.9}$$

S_f and S_m are sink terms for both regions and is the transfer rate for water from inter to the intra aggregate pores.

The mass transfer rate, Γ_w, for water between the fracture and matrix regions is assumed to be proportional to the difference in effective water contents of the two regions using a first order rate equation

$$\Gamma_w = \frac{\partial \theta}{\partial t} = \omega[S_e^f - S_e^m] \tag{2.10}$$

where ω is a first order rate coefficient (T^{-1}). Compared to a pressure head based driving force, the dual porosity model based on the mass transfer equation requires significantly fewer parameters since one does not need to know the retention function for the matrix region explicitly, but only its residual and saturated water contents.

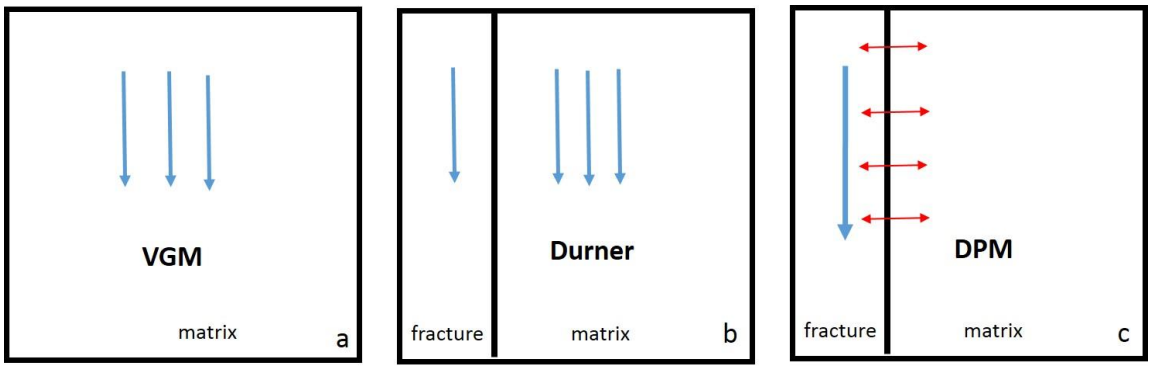

Figure 1: Schematic representation of van Genuchten (VGM), Durner and Dual Porosity (DPM) conceptual models. Arrows represent water flow in porous media matrix and fractures.

2.3 Study Area

Soil samples were collected during the Southern Great Plains 1997 (SGP97) Hydrology Experiment [*Mohanty et al.*, 2002] in the Little Washita watershed, Oklahoma, USA. The Little Washita watershed covers 610 km^2 and is a tributary of the Washita River in Southwest Oklahoma as seen in Figure 2 (used with permission from *Das, Narendra N.*, 2005). Mostly, the climate in region is classified as sub-humid [*Allen and Naney*, 1991; *Famiglietti et al.*, 1999]. Summers are typically long, hot and relatively dry and winters are typically short, temperate and dry but are very cold for a few weeks. Much of the annual precipitation and most of the large floods occur in the spring and fall [*Allen and Naney*, 1991]. This region has a moderately rolling topography and the soil is comprised of a wide range of textures which includes both coarse and fine soils [*Schwarz and Alexander*, 1995; *US Natural Resources Conservation Service*, 1995]. Soils in this watershed are closely related to the composition of the underlying bedrock. Roughly half of the watershed has a fine texture with fine sand and loamy fine

sand. The remainder of the watershed area, soil consists of sandy loam, loam and silt loams. Small part of the watershed also consists of clayey soils (Ffigure 3). The upland topography of this region is gently to moderately rolling. The alluvial areas have the flattest slopes, usually 1 percent or less. The channel system is well developed throughout the watershed and almost extends to the drainage divide in most areas [*Allen and Naney*, 1991].

A total of 157 soil cores were collected across the watershed for soil hydraulic property experimental and numerical studies. Soil cores (in brass cylinders, 5.2 cm diameter and 5.9 cm long) at different depths were collected from representative soil, slope and vegetation, during the SGP 97 hydrology experiment. Out of 157 soil samples, we carefully selected 50 samples for this study. These 50 samples include all major soil types, topography, organic matter, vegetation and soil depth (varying from 5cm to 90cm from soil surface) as shown in Figure 3. Figure 4 shows the variety of soil textures used in this study in relation to the USDA soil textural triangle. Figure 5 shows the locations of soil samples in the digital elevation model (DEM) of the watershed, which was developed using ArcGIS. Table 1 shows the details of 50 soil samples including soil type, depth from land surface, landscape position, vegetation type and organic matter content used in this study. More details of SGP 97 experiment datasets are available in *Mohanty et al.* [2002].

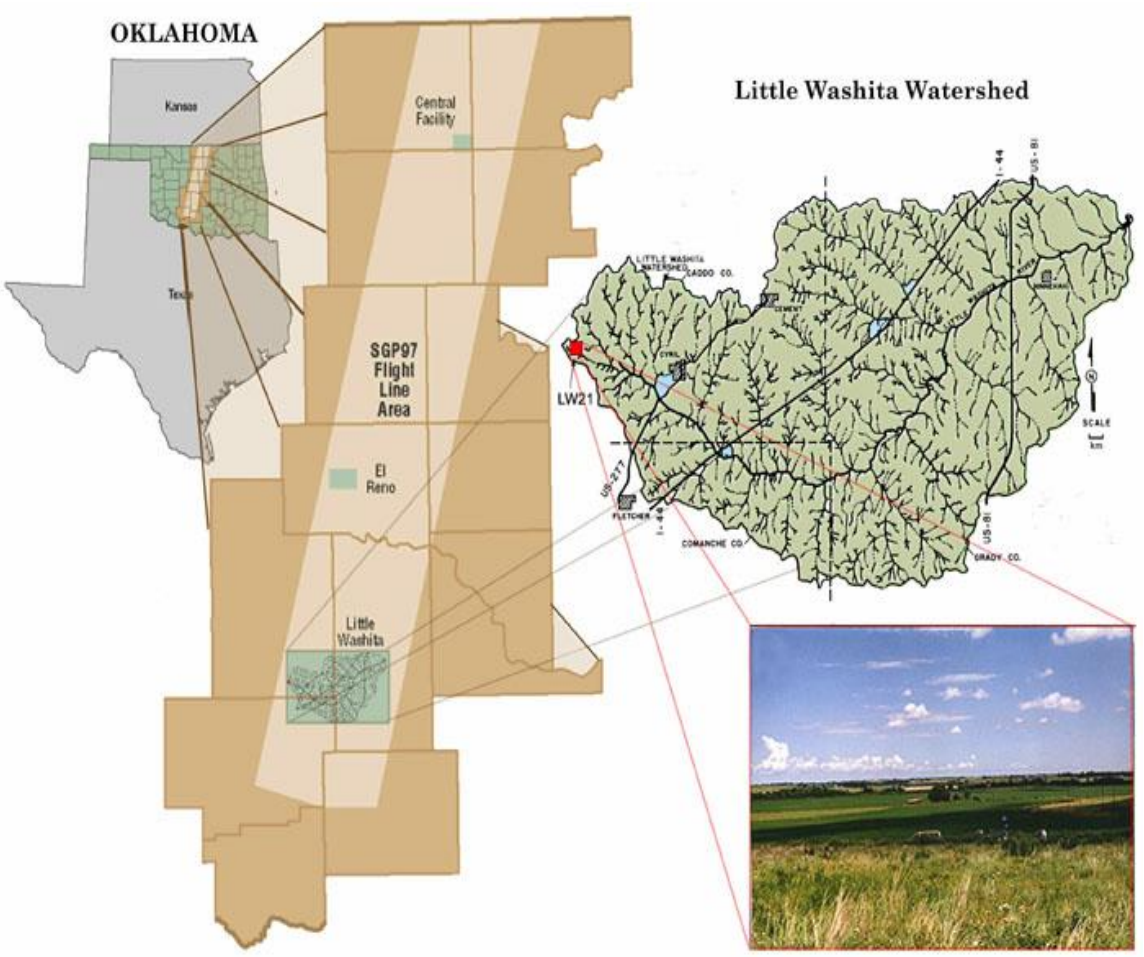

Figure 2: The Little Washita watershed, Oklahoma, USA [Das, 2005]. A typical field in the watershed shown in the inset. SGP 97 flight line area shows the extent of airborne remote sensing soil moisture data collected during the field campaign.

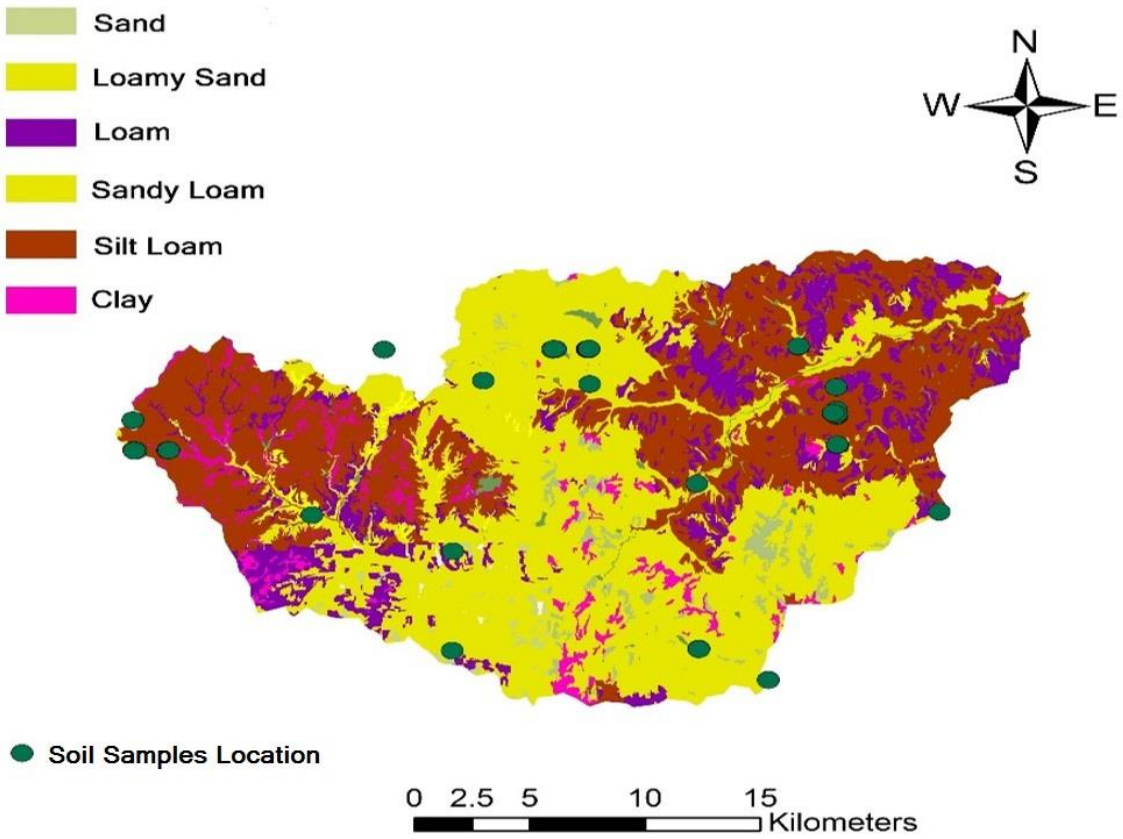

Figure 3: Soil texture across the Little Washita watershed, SSURGO

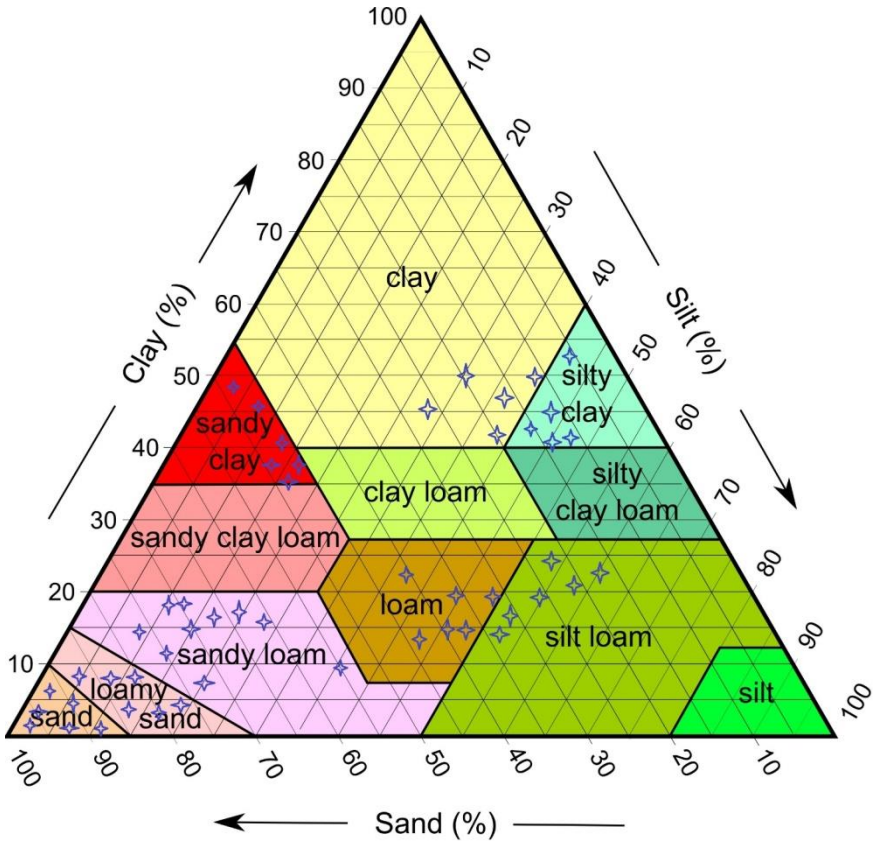

Figure 4: Soil samples (marked in blue) used for the study are shown on the USDA soil textural triangle.

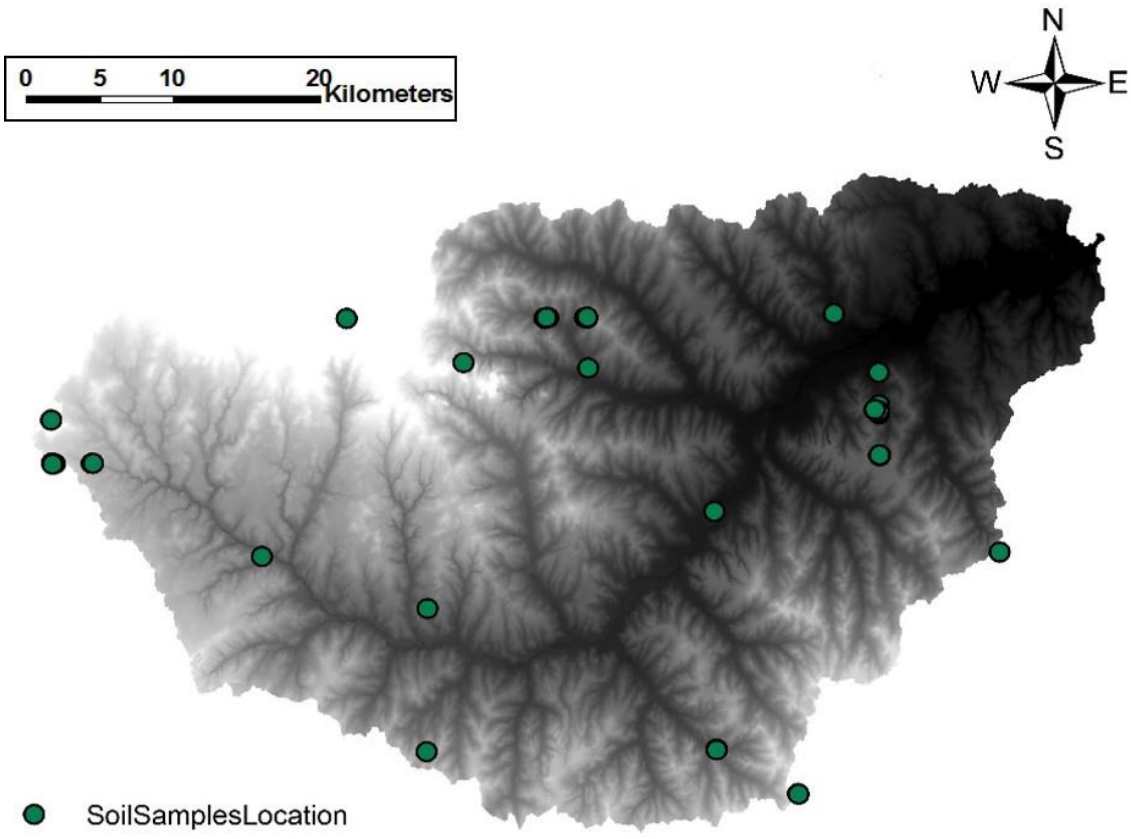

Figure 5: Locations of soil samples used in the study are shown in green on a digital elevation model of Little Washita watershed.

Table 1: Details of 50 soil samples used for the study including soil type, depth from surface, landscape position, vegetation type and organic matter content.

Sample ID	Soil type*	Soil Depth (cm)	Landscape Position	Vegetation Type	Organic Matter (%)
5	L	0-30	Valley	Grass	0.96
7	L	60-90	Valley	Grass	0.38
8	L	70-75	Valley	Grass	0.38
12	LS	3-9	Hilltop	Pasture	0.4
13	SL	3-9	Hilltop	Pasture	0.15
15	S	3-9	Slope	Pasture	0.3
16	S	3-9	Slope	Pasture	0.38
17	SL	6-12	Valley	Pasture	0.46
21	SL	0-30	Mid-slope	Pasture	0.29
23	SL	53-59	-	-	0.25
24	LS	3-9	Hilltop	Pasture	0.66
26	SCL	13-18	-	-	0.42
29	LS	3-9	Mid-slope	Pasture	0.72
32	SL	3-9	Mid-slope	Grass	0.5
35	SCL	19-25	Top of crest	Pasture	0.73
36	SCL	40-46	Top of crest	Pasture	0.44
37	SCL	60-90	Top of crest	Pasture	0.16
38	SL	3-9	Mid-slope	Grass	0.37
39	SL	3-9	Mid-slope	Grass	0.49
41	S	23-29	Valley	Grass	0.13
54	L	38-44	Flat Field	Grass	0.41
55	SiL	73-79	Flat Field	Grass	0.3
58	SiL	3-9	Bottom	Pasture	1.51
67	SCL	3-9	Mid-slope	Pasture	1.11
69	LS	3-9	Flat Land	Pasture	0.84
70	S	3-9	Mid-slope	Pasture	0.27
71	S	3-9	Near Top	Pasture	0.26
73	LS	3-9	Slope	Pasture	0.47
74	LS	3-9	Top of Ridge	Pasture	0.61
75	S	3-9	Hilltop	Pasture	0.36
78	SL	20-40	Flat	Pasture	0.4
79	SL	40-60	Flat	Pasture	0.4
88	CL	28-34	Valley	Pasture	1.74
100	SiCL	48-54	Flat Field	Winter Wheat	0.71
101	CL	73-79	Flat Field	Winter Wheat	-
102	CL	93-99	Hilltop	Winter Wheat	0.46
104	SiCL	53-59	Flat Field	Pasture	0.62
105	SiC	83-89	Flat Field	Pasture	0.38
108	SiL	3-9	Valley	Winter Wheat	0.66
109	SiL	33-39	Valley	Winter Wheat	1.56

Table 1 continued

Sample ID	Soil type*	Soil Depth (cm)	Landscape Position	Vegetation Type	Organic Matter (%)
110	CL	53-59	Flat Field	Winter Wheat	0.67
111	CL	76-82	Flat Field	Winter Wheat	0
113	L	3-9	Hilltop	-	0.37
114	SiL	3-9	Hilltop	Pasture	1.76
115	CL	3-9	Slope	Pasture	0.78
116	L	3-9	Slope	Pasture	0.75
151	SiC	3-9	Valley	-	-
152	SiCL	3-9	Valley	-	-
153	SiCL	3-9	Valley	-	-

where: L: Loam LS: Loamy Sand SL: Sandy Loam
SCL: Sandy Clay S: Sand SiCL: Silt Clay CL: Clay

2.4 Methodology

2.4.1 Experimental Setup

According to [*Durner et al.*, 1999], inflow/outflow experiments provide sufficient information to uniquely identify parameters of the retention function and the unsaturated conductivity function. Over the years, classical one step outflow methods have performed poorly. Although, optimization of the parameters describing the SHPs in an outflow experiment is a promising method to derive SHPs but estimates from one step outflow experiments using cumulative outflow data in the objective function are often unreliable and non-unique. Multistep outflow method was introduced by [*Eching et al.*, 1994; *Van Dam et al.*, 1994] which uses a sequence of smaller pneumatic pressure increments to induce drainage of soil core. Applied pressures were -5, -10, -20, -40, -80, -120, -160, -333, -1000, -3000, -8000 and -15000 cm. Soil water retention data points were obtained by calculating water balance in the soil sample at each pressure head step of the experiment.

We used the soil samples for conducting a multi-step outflow (MSO) experiment. Multistep outflow experiments evaluated by inverse modeling is an efficient way to determine simultaneously the water retention and hydraulic conductivity functions of soil [*Eching et al.,* 1994; *Van Dam et al.,* 1994]. This approach is based on transient experiments where a porous medium sample is saturated with water and then drained by decreasing the boundary pressure stepwise, e.g., matric potential at the lower boundary. The use of outflow experiment for estimation of SHPs is advantageous because it is flexible with its initial and boundary conditions [*Eching and Hopmans,* 1993; *Eching et al.,* 1994]. These methods have become very popular to study the phenomenon of non-equilibrium water flow in variably saturated porous media with the advancement of computing speeds to determine the soil hydraulic properties [*Figueras and Gribb,* 2009; *Laloy et al.,* 2010; *Puhlmann et al.,* 2009].

The experimental procedure involves the measurement of cumulative outflow and soil water pressure head as a function of time from initial near saturated soil cores. The MSO experimental setup has been described in detail by *Tuli et al.* [2001], and our experimental setup is shown in Figure 6 and Figure 7.

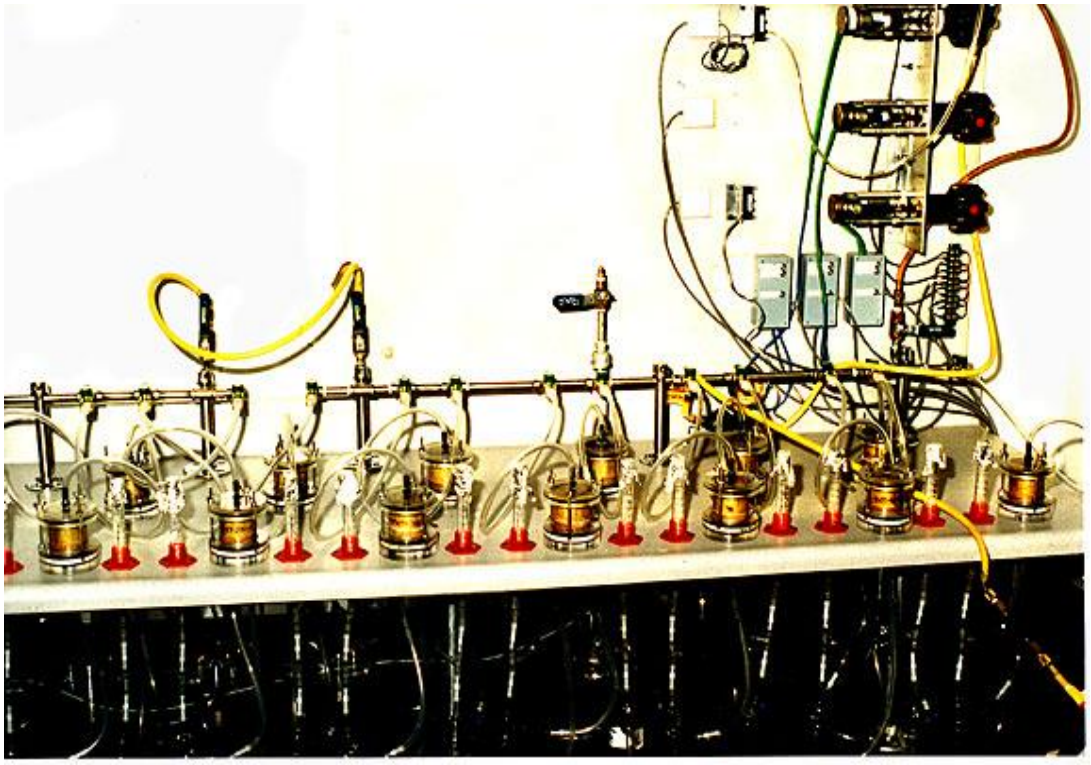

Figure 6: Experimental set-up of multistep outflow experiment conducted on soil samples which were collected during the SGP 97 hydrology experiment.

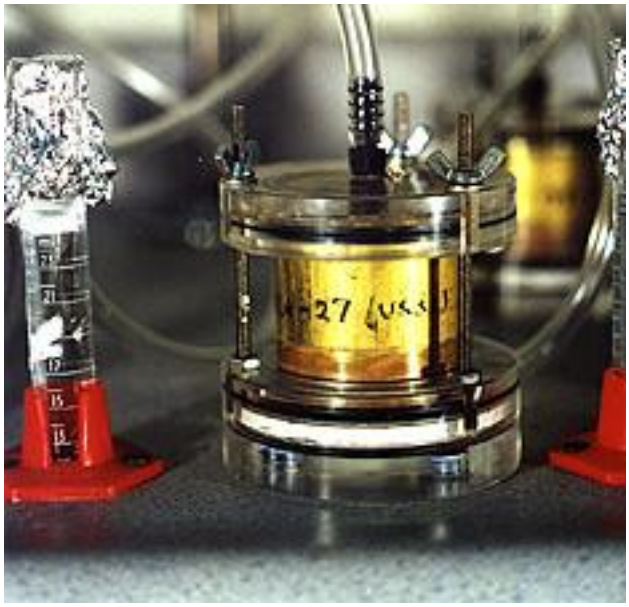

Figure 7: Zoom in view of a single soil sample, during the multi-step experiment.

2.4.2 Modeling Framework

2.4.2.1 Inverse Estimation of Parameters

Hydrus-1D [*Šimůnek et al.,* 2008] was used for all simulations. Single porosity and dual porosity models with water transfer functions were used to simulate flow. In these models infiltration and drainage experiments were described by fitting the numerical solution of Richards' equation. Measured saturated hydraulic conductivity values were used as initial estimate in all simulations. For other parameters, the initial values were generated based on neural network based pedo-transfer functions by *Schaap et al.* [2001] based on soil type built within HYDRUS 1D modeling framework. The range of parameter values for single porosity (VGM), bimodal (Durner) and dual porosity models (DPM) are shown in Table 2. Five parameters (θ_r, θ_s, α, n, K_s and l) are related to VGM. Besides VGM parameters, w_2, α_2 and n_2 are used in Durner's model. In DPM, along with VGM parameters θ_{rlm}, θ_{slm} and ω are parameterized in local optimization. All ranges vary according to the soil type. In single porosity model, four parameters were estimated inversely where parameter l (describing tortuosity) was fixed at 0.5. Combination of dynamic multistep experiment data with static retention data was used (with weights 1 and 10 respectively) to improve the performance of optimization.

In Durner's model, besides the four VGM parameters, three more parameters (α_2, w_2, n_2) were inversely calculated. Water flow in dual porosity model requires the same parameters as in the single porosity model in the mobile region plus three other parameters for the immobile region: θ_{rlm}, θ_{slm}, and ω. The additional parameters of the dual porosity model, although complicated, were expected to better represent the macro-

pore flow processes than the single porosity model. Additionally, ‘constant flux’ and ‘variable pressure head’ were assumed as the top and bottom boundary conditions respectively. An example of the Hydrus 1D [*Šimůnek et al.,* 2008] domain setup is shown in Figure 8. In our simulation, the laboratory measured saturated hydraulic conductivity (K_{sat}) of the ceramic plate at the bottom boundary were fixed at their respective values. Figure 8 also shows the pressure head initial conditions which were taken as -6.4 cm and -1 at the top and bottom nodes, respectively.

2.4.2.2 Simulation Models

Firstly, the single porosity VGM model [*Van Genuchten,* 1980; *Mualem,* 1976] was used to assess the water flow through unsaturated soil in the soil core using cumulative outflow and water retention data from the multistep experiments. Secondly, a bimodal dual porosity model [*Durner,* 1994] and non-equilibrium dual porosity flow model, DPM, where mass transfer between the mobile and immobile zones assumed to in water flow simulation. Table 3 shows the water flow models and their governing equations, which are shown in first and third column respectively. Last column indicates the number of parameters which were optimized in simulations. In Hydrus-1D, the Galerkin-type linear finite element method was used for spatial discretization of the governing partial differential equations, while finite difference methods were used to approximate temporal derivatives.

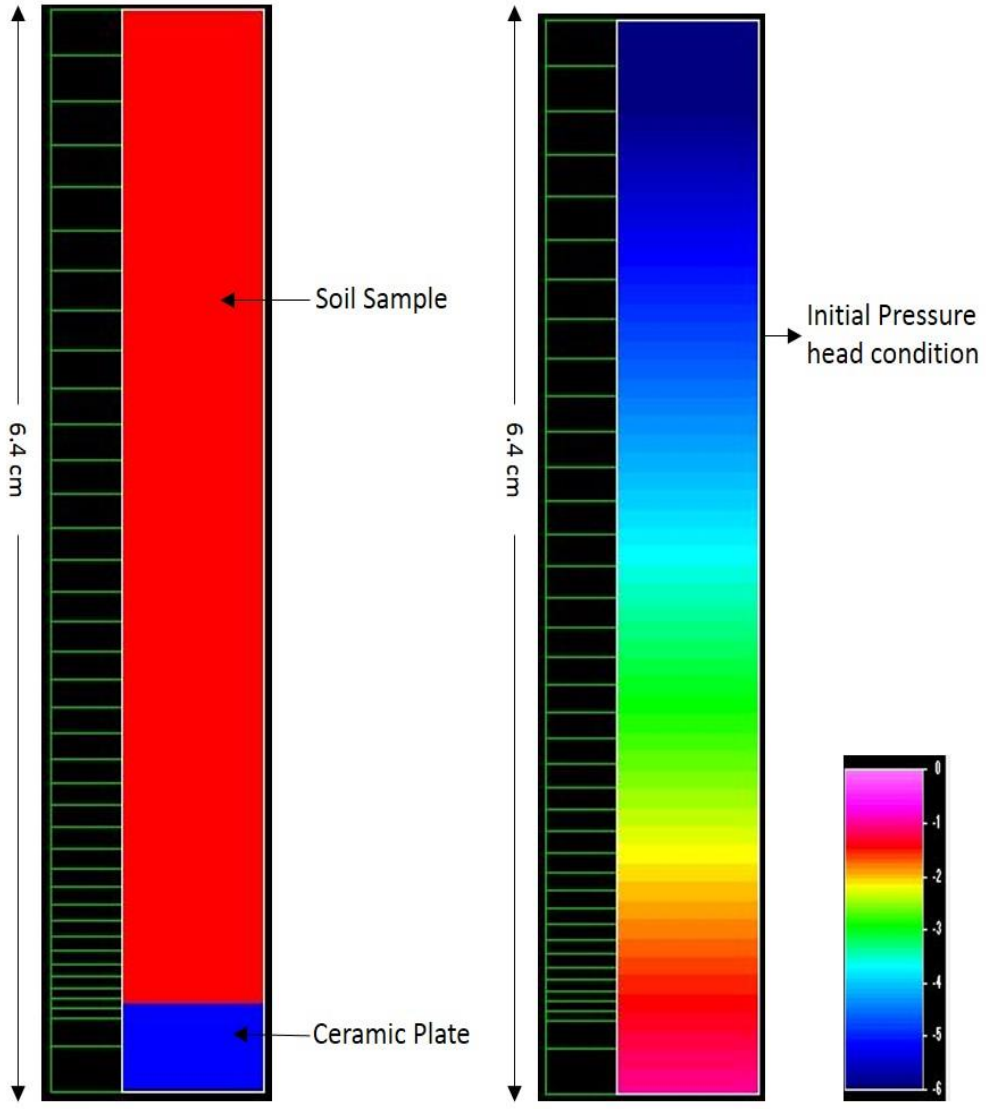

Figure 8: Left: Hydrus 1D soil domain profile with two materials. Material 1, shown as red, is the soil. Material 2, shown in blue at the bottom boundary is a ceramic plate. Right: Initial (pressure head) conditions.

Table 2: Range of parameter values for (a) single porosity and (b) bimodal and (c) dual porosity models. θr, θs, α, n, Ks and l are parameters related to VGM. Besides VGM parameters, w_2, α_2 and n_2 are used in Durner's model for parameterization. In DPM, along with VGM parameters, θ_{rlm}, θ_{slm} and ω are parameterized. All ranges vary according to the soil type.

Parameter	Range	Definition
(A) Single Porosity		
θ_r	0-0.2 (cm^3/cm^3)	Residual soil water content
θ_s	0.21-0.6(cm^3/cm^3)	Saturated soil water content
α	0-0.1(1/cm)	Empirical coefficient in soil water retention function
n	1.1-2.5 (-)	Empirical coefficient in soil water retention function
K_s	measured value	Saturated hydraulic conductivity
l	0.5	Tortuosity parameter in the conductivity function
(B) Durner Model		
θ_r	0-0.2 (cm^3/cm^3)	Residual soil water content
θ_s	0.21-0.6(cm^3/cm^3)	Saturated soil water content
α	0-0.1(1/cm)	Empirical coefficient in soil water retention function
n	1.1-2.5 (-)	Empirical coefficient in soil water retention function
K_s	measured value	Saturated hydraulic conductivity
l	0.5	Tortuosity parameter in the conductivity function
w_2	0-1 (-)	Relative weighting factor for the subcurve for the second overlapping subregion
α_2	0-1 (1/cm)	Second empirical coefficient in soil water retention function
n_2	1-3 (-)	Second empirical coefficient in soil water retention function
(C) Dual Porosity		
θ_r	0-0.2 (cm^3/cm^3)	Residual soil water content
θ_s	0.21-0.6(cm^3/cm^3)	Saturated soil water content
α	0-0.1(1/cm)	Empirical coefficient in soil water retention function
n	1.1-2.5 (-)	Empirical coefficient in soil water retention function
K_s	measured value	Saturated hydraulic conductivity

Table 2 continued

Parameter	Range	Definition
l	0.5	Tortuosity parameter in the conductivity function
θ_{rlm}	0.01-0.1 (cm^3/cm^3)	Residual water content in immobile domain
θ_{slm}	0-1 (cm^3/cm^3)	Saturated water content in immobile domain
ω	0-1 (cm^3/cm^3)	Mass transfer coefficient for loamy soil

Table 3: Water flow models used in this study with the type and their governing equations. Last column shows the number of optimized parameters in inverse modeling.

Model Name	Model Type	Water Flow Equation	No. of optimized parameters
VGM	Single Porosity	[2.1], [2.2], [2.3]	4
Durner	Dual Porosity	[2.1], [2.5], [2.6]	7
DPM	Dual Porosity	[2.7], [2.8], [2.9], [2.10]	7

* Measured K_{sat} values were used in optimization and l is fixed at 0.5

2.4.2.3 Model Parameterization and Strategy

The inverse parameter estimation was performed by Levenberg–Marquardt nonlinear minimization of the objective function Φ:

$$\varphi(\boldsymbol{b}) = \sum_{j=1}^{m} v \sum_{i=1}^{n} w_{i,j} \left[O\left(x, t_i\right) - E\left(x, t_i, \boldsymbol{b}\right)\right]^2 \qquad (2.11)$$

where m is the total number of measurements; n is the number of observations in a particular measurement set; $O_j(x,t_i)$ is the observation at time i for the jth measurement set at location x; $E_j(x,t_i,b)$ are the corresponding estimated space time variables for the vector $\boldsymbol{b}$ of optimized parameters from the respective numerical model used for water flow through saturated soil in porous media; and v_j and $w_{i,j}$ are weighting factors associated with a particular measurement set or point, respectively. In this study, $w_{i,j}$ were set equal to 1 assuming similar error variances within a particular measurement set. Only data that are measured at larger time intervals and are underrepresented with respect to more frequent measurements require weights wi,j. Then, v_j is calculated for each simulation as [*Clausnitzer and Hopmans,* 1995]

$$v_j = \frac{1}{n_j \sigma_j^2} \qquad (2.12)$$

which assumes that v_j is inversely related to the variance σ_j^2 within the jth measurement set and to the number of measurements n_j within the set.

From our dataset, the soil hydraulic parameters of each soil sample were estimated using cumulative outflow data from multistep experiment. To make our results more robust, we added retention data with a higher weight. Improvements were observed by adding retention data to the cumulative outflow data.

2.4.2.4 Goodness-of-fit Criteria

We inferred the results statistically for direct comparison between various models and for evaluating best fit of parameters in inverse analysis. Mean absolute error (MAE), root mean square error (RMSE) along with Akaike information criterion (AIC) and Bayes information criterion (BIC) were used for inferring the results. An absolute error measure like the *MAE* carries the same units as the observations and is able to better assess the magnitude of deviation. A lower *MAE* typically signifies better agreement between modeled and observed values.

$$MAE = \frac{\sum_{i=1}^{N}[|O_j(x,t_i) - E_j(x,t_i,\boldsymbol{b})|]}{N} \tag{2.13}$$

A higher coefficient of determination and lower sum of squares error typically signify better agreement between prediction and observation. For our analysis, R^2 >0.9, SSE <100 (two-orders of magnitude difference between observed and predicted values are selected as the acceptable criteria for judging performance of continuum-scale models and inverse estimation of parameters. The performance of three models has also been quantified using AIC and BIC which can be used to decide which of the three models is most favored for the available soil samples. These two measures are defined through the following information criterion

$$I_i = -2\ln(L_{\max,i}) + \xi(p_i) \tag{2.14}$$

Where L_{max} is the maximum likelihood of model *i* and $\xi(p_i)$ represents a penalty term that penalizes for the number of parameters, *p* [*Diks and Vrugt,* 2010]. The AIC and BIC

diagnostics trade off quality of fit against the model complexity. If the residuals are Gaussian distributed, the value of L_{max} can be computed from the SSE using

$$-2\ln L_{\max} = N_s \ln\left(\frac{SSE}{N_s - 1}\right) + N_s \tag{2.15}$$

where N_s is the number of observations. The penalty term for AIC is $\xi(p)=2p$ and for BIC this term is given by $\xi(p)=p\ln(N_s)$. The model with the lowest values for AIC and/or BIC is most supported by the available data. Note that AIC and BIC typically uses the number of ‘‘calibration’’ parameters as measure of model complexity (penalty term).

2.4.3 Forward Modeling for Soil Moisture Prediction

The calculated SHPs of the selected soil samples from inverse modeling were used to calculate soil moisture by forward modeling. Using time invariant soil properties, we calculated and compared soil moisture which is a time dependent property. The forward modeling was done by using Hydrus-1D. HYDRUS may be used to simulate movement of water, heat and multiple solute in variably saturated media. This program uses linear finite elements to numerically solve the Richard’s equation for saturated-unsaturated water flow and Fickian-based advection dispersion equations. We again used VGM, Durner and DPM to run simulations to calculate soil moisture. A 100 cm domain was setup up, using HYDRUS-1D, as shown in Figure 9 with a single soil layer. Observations nodes were at 5, 25, 60 cm and 75 cm from the surface. The simulation was run from March 1997 to November 1997 (245 days), around the SGP 1997 Hydrology experiment (June 18-July 18, 1997). As soil moisture prediction would

highly depend on antecedent soil moisture therefore, initial water content from February 28, 1997 were used as initial conditions which was available from Oklahoma Mesonet (http://www.mesonet.org/). Atmospheric boundary condition with surface runoff as the top boundary condition was used. The potential water flux across the upper boundary is controlled by external conditions. However, the actual flux depends also on the prevailing (transient) soil moisture conditions. The soil surface boundary condition may change from a prescribed flux to a prescribed head type condition and vice-versa. Free drainage was used as a bottom boundary condition. A zero gradient boundary condition can be used to simulate a freely draining soil profile. This boundary condition replicates field conditions of water flow and drainage in vadose zone. As water table much below than 100cm in Oklahoma, this kind of bottom boundary condition was used in our study. Feddes [1977] root water uptake model was used to simulate plant water use. Other meteorological conditions (forcing) such as precipitation, daily average temperature, humidity, wind speed and radiation were obtained from Mesonet (http://www.mesonet.org/) for the study duration.

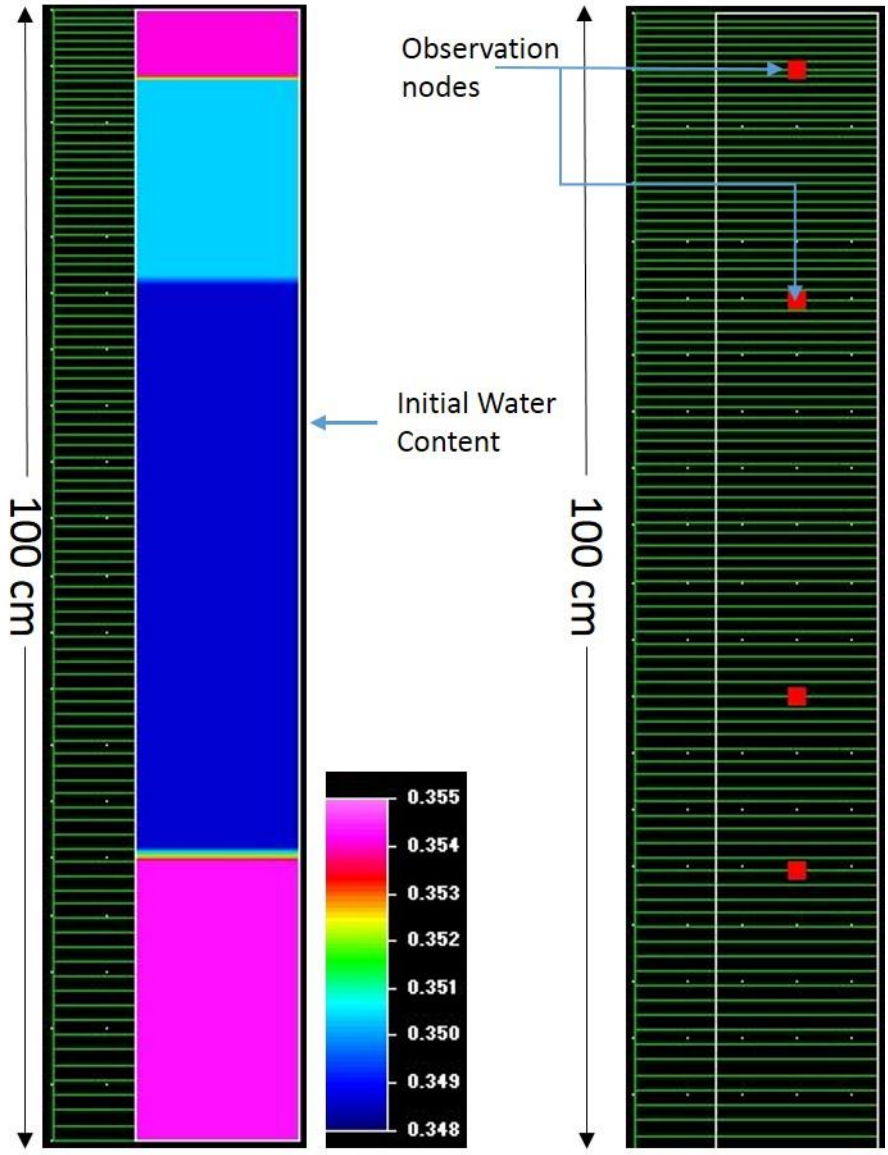

Figure 9: Forward modeling domain setup in HYDRUS-1D. On the left, initial condition (in terms of water content) is shown.

2.5 Results and Discussions

2.5.1 Inverse Modeling

The soil hydraulic parameters were inversely estimated using single porosity (VGM), Durner's model, and dual porosity model (DPM). Our study was based on simulations which were run on experimental multistep data under monotonic imbibition or drainage histories. The experiment also accounted for dynamic outflow which enabled us to incorporate some non-equilibrium effects in inverse modeling. Non-equilibrium in our study was observed as apparent non-uniqueness of the relationship between water content and pressure head under hydrostatic steady state, or monotonically changing hydraulic conditions. Observed and simulated cumulative outflow data for two (randomly selected) soil samples (out of 50 samples selected for the study) are shown in Figure 10 and Figure 11, where simulated pressure head obtained from three models were a good match, but cumulative outflow was described differently. Dynamic non-equilibrium was observed in cumulative outflow in multistep experimental data. A large fraction of water drains quickly from the column directly after each pressure step (as shown by the 'steps' in the observed outflow) followed by a phase of continuing slower outflow. The estimated soil hydraulic parameters reproduce sufficient details to infer how different numerical models bring out the variability because of the soil texture and structure and underlying physical processes. During the initial phase of the multi-step outflow experiment or at the wet end, these differences between the models are very prominent. The dual porosity and VGM models are able to better capture the large outflow values immediately after the pressure is dropped, than the Durner model. Using

results similar to Figure 10 and Figure 11 as a reference, based on RMSE values, we observed that overall the dual porosity model was able to capture the flow pattern better than bimodal Durner's and single porosity VGM model. We also noticed that estimation of soil hydraulic parameters was dependent not only on the matric potential but was also influenced by the (dynamic) outflow rate and the pore size distribution. Using similar experimental data, *Diamantopoulos et al.* [2012] reported that the MSO experiments are bound to have dynamic effects. Further, they recognized two separate phases in the outflow dynamics. In the first phase, water drained abruptly from the column directly after each pressure step, as expected in equilibrium relationship with the capillary pressure dynamics. However, in a second phase, outflow continued and ceased only slowly.

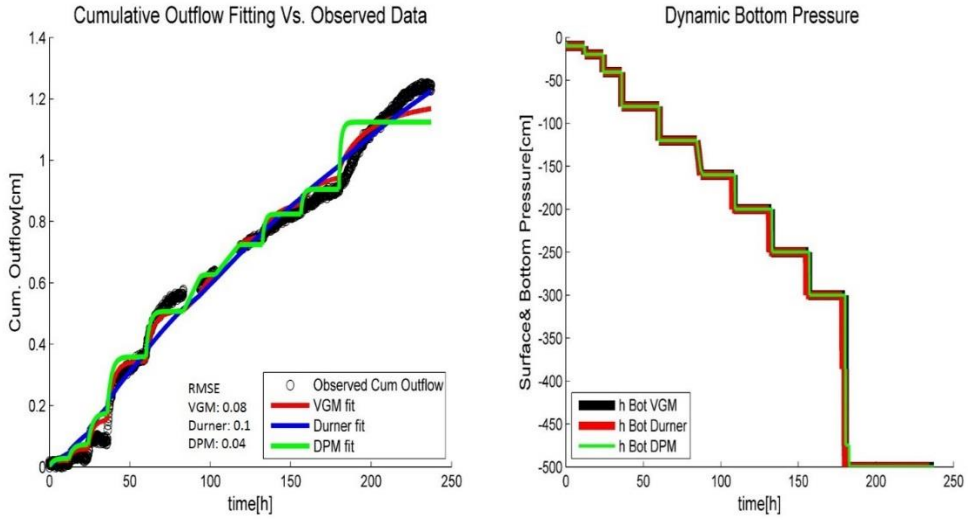

Figure 10: Observed and simulated cumulative outflow and pressure head for a loamy sand soil. The fitted data were calculated using VGM, Durner and DPM models.

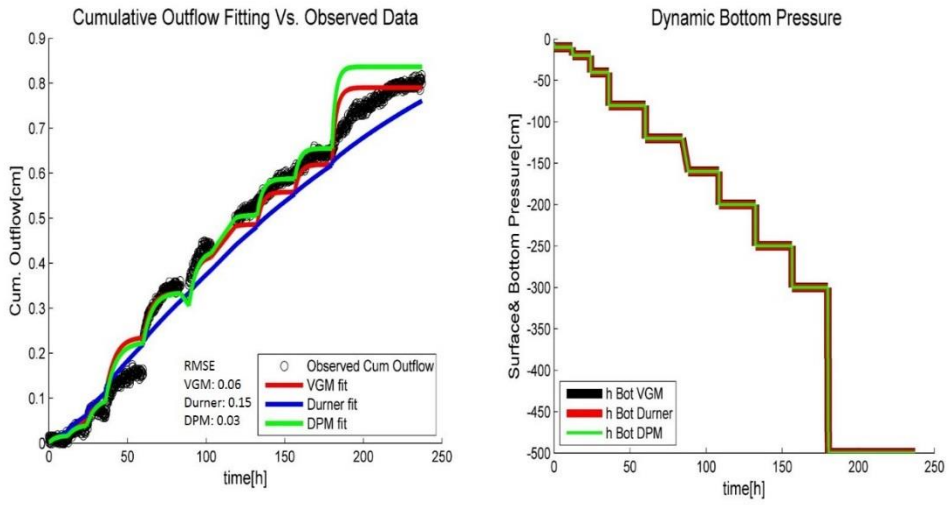

Figure 11: Observed and simulated cumulative outflow and pressure head for a clay soil. The fitted data were calculated using VGM, Durner and DPM models.

A number of continuum scale physical processes could have affected the outflow during the multistep experiment, which is evident in the soil water retention and hydraulic conductivity functions. Physical processes controlling outflow such as entrapment of water, pore water blockage, air entrapment and air entry value can be considered as the reason of variation in outflow from different soil cores. These phenomenon leads to variable drainage rate which directly affects retention property and hydraulic conductivity of soil samples. We believe at continuum scale soil texture is the most dominant feature affecting the outflow. Besides these effects pore size distribution and pore connectivity result in non-equilibrium hydraulic effects.

2.5.2 Parameter Identification and Uniqueness

The metrics used to evaluate the validity of each model were R^2, MAE and RMSE. To complement we also used AIC and BIC to explicitly recognize the differences in the number of input parameters on the model fitting. These statistical parameters are calculated for various soil types (Figure 12). We observed that dual porosity model outperforms Durner and van Genuchten model with the least RMSE value. In our tests, lowest AIC and/or BIC values support the model but BIC penalizes the number of parameters in the model to a greater extent than AIC, as shown in Figure 13. So we would more rely on RMSE and BIC values. AIC and BIC for clay, loam, loamy sand, sand, sandy clay and sandy loam are show in figure 13. Calculated SHPs are supported by R^2, MAE, RMSE, AIC and BIC. Our derived SHPs are consistent with RETC [*Van Genuchten et al.,* 1991] and UNSODA [*Leij,* 1996; *Nemes et al.,* 2001] soil hydraulic properties database. We observed that estimation of SHPs using different models based on soil texture were similar in many soil samples, which necessitates the requirement of consideration of other factors such as topography, vegetation and organic matter content in describing water flow in (structured) soils in various landscape positions.

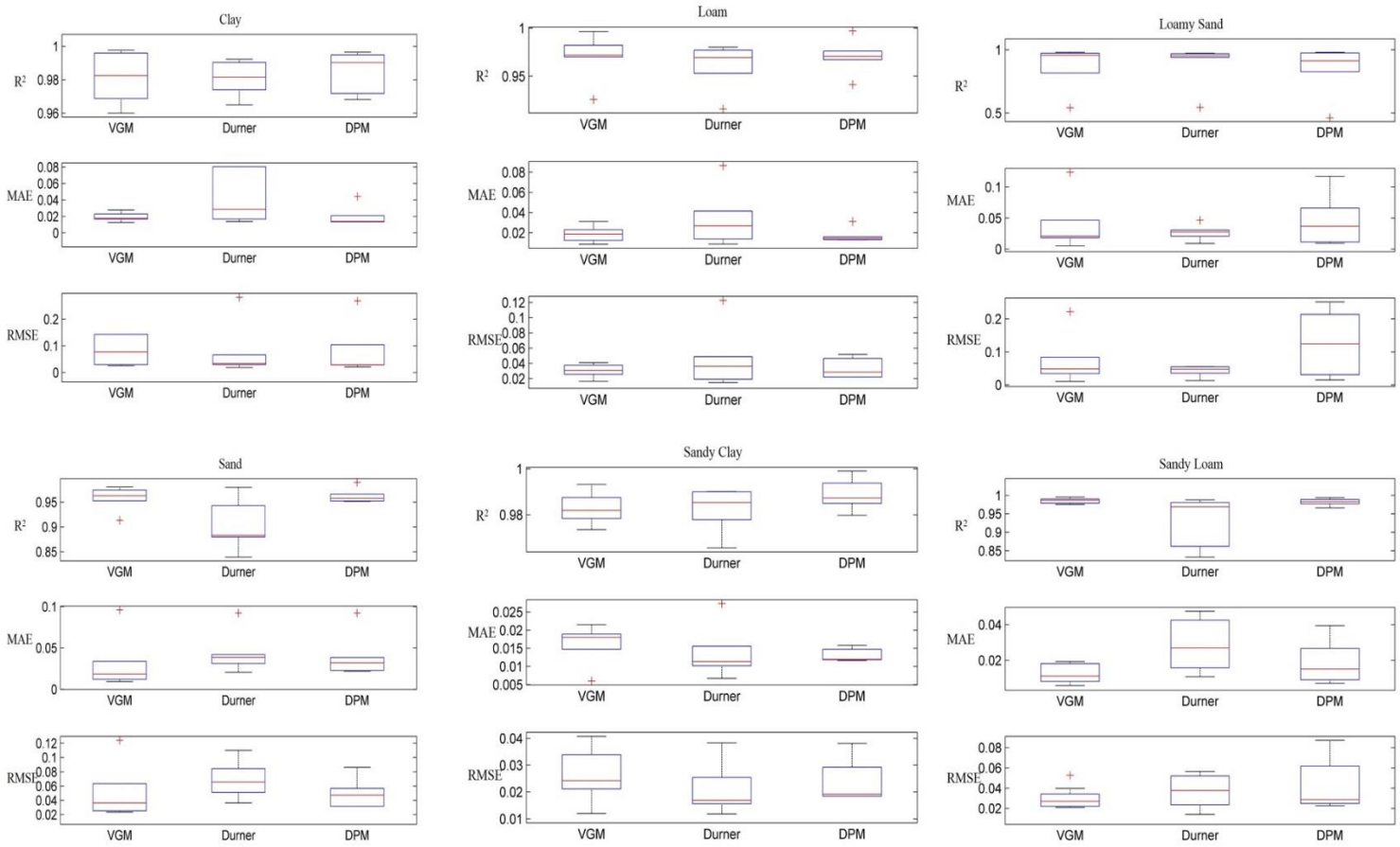

Figure 12: Inverse modeling statistical fitness are shown for selected 50 soil samples. R^2, MAE and RMSE for soil samples in different soil types including clay, loam, loamy sand, sand, sandy clay and sandy loam.

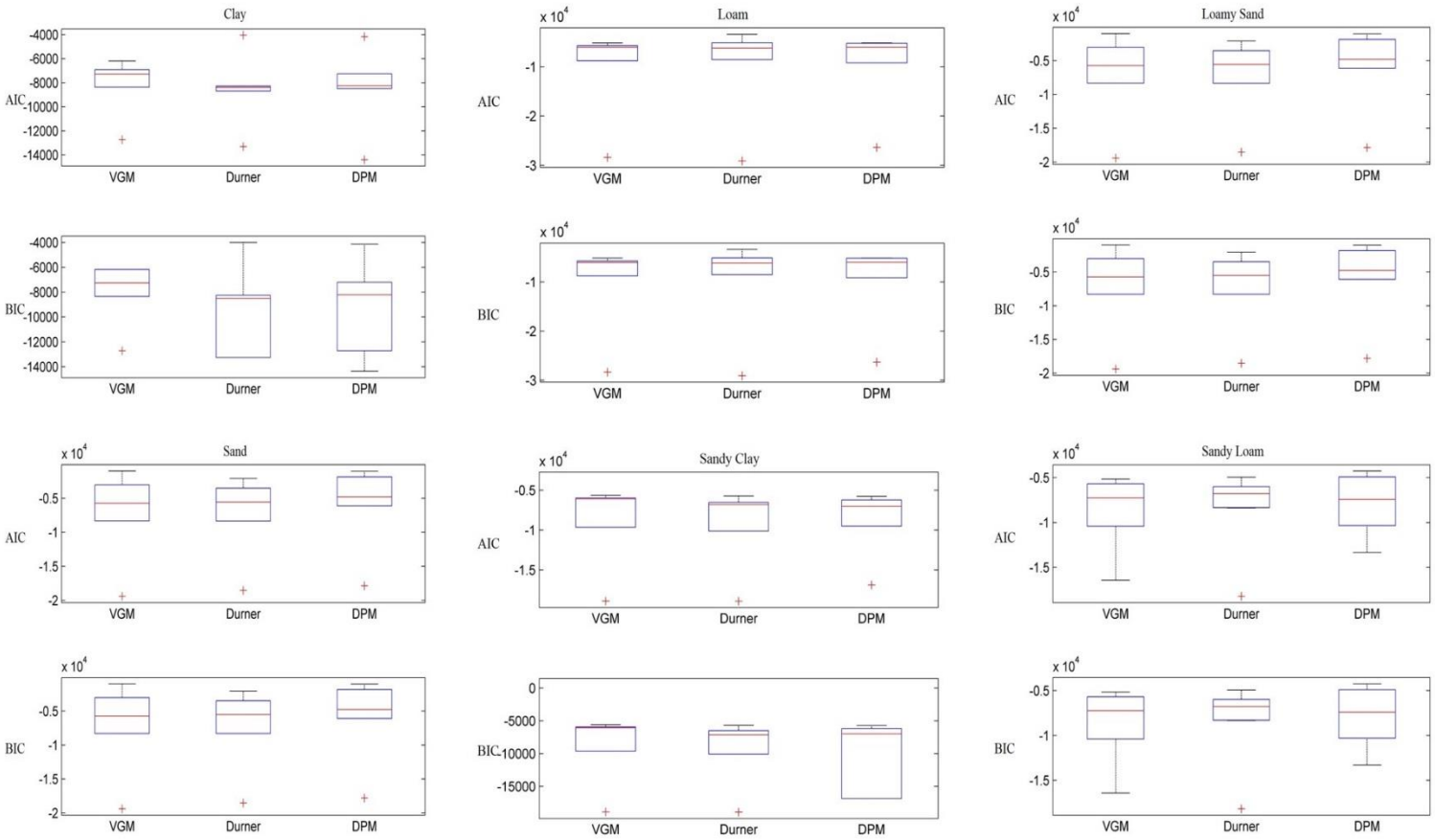

Figure 13: Statistical parameters, AIC and BIC are shown for 50 selected soil samples. Soil types include clay, loam, loamy sand, sand, sandy clay and sandy loam.

SHPs calculated from inverse modeling are used to plot soil water retention and hydraulic conductivity functions for various soil samples. They represent soil samples which differ in soil type, soil depth, organic content and topography within the Little Washita watershed. Representative retention curves of different soil types, depth, organic content and topography are shown in Figure 14-17. Similarly, representative hydraulic conductivity functions of various samples shown in Figure 18-21. Both soil water retention curves and hydraulic conductivity functions are plotted using the three models (VGM, Durner and DPM). Even though at the same pressure head, the same amount of water might be stored but the flow regime leading to that water content distribution varies because of difference in hydraulic conductivity functions. As discussed earlier, these three models are structurally different and predict unsaturated soil water flow differently among which heterogeneity is a major factor. The heterogeneity at field scale could be because of various reasons like soil type, topography, soil organic matter, and soil depth.

Matrix-fracture interfaces can have very different properties than the bulk matrix due to the deposition of organic matter which can reduce rates of water flow between macropores and the soil matrix [*Thoma et al.,* 1992] and increase water retention. Near dry region in fine soils, the retention curve is best described by DPM as the crack volume in dry clay soils can be substantial, especially in the surface layers as shown in Figure 17. We confirm our results with [*Messing and Jarvis,* 1990; *Lin et al.,* 1998] that near saturated and saturated hydraulic conductivity in clay soils are positively correlated to macroporosity and inversely related to the soil moisture content. Topography exerts a

strong control on distribution of soil particles, which in turn strongly influences soil hydraulic properties. Topography plays an important role in determining the soil texture, soil depth, and vegetation attributes at any landscape position (location) which together determine the soil pore structure. In this study, we have considered three landscape positions, including hill-top, valley and slope. Soil erosion causes greater amount of fine particles to be present in valleys as opposed to hill-top. *Beke and MacCormick* [1985] made it evident that employing organic matter into soil water retention studies are useful. *Hollis et al.* [1977] proved that presence of organic matter could be useful in estimating soil water content. Presence of organic carbon affects soil composition and adsorption properties and the relationship of soil water retention to organic carbon is affected by proportions of textural components [*Rawls et al.*, 2003]. Therefore, variation in organic carbon content affects soil water retention and SHPs leading to soil water content distribution at different landscape positions.

In figure 17, two soil samples collected from different locations across the watershed are presented. On the left, the soil sample with 0.46% organic carbon and hilltop topography whereas the soil sample on the right has 0.78% organic carbon with slope topography. Although, soil type (clay) remains same for both samples, topography and organic matter content affect the soil hydraulic properties. The DPM model does not predict water content effectively for the sample with higher organic carbon and flat topography. This difference is especially highlighted at the dry end where the water content is underestimated with respect to the other two models. This may suggest because DPM model quickly loses water at the wet end and dries out quicker than the

other two models. However, under actual field conditions, the high organic matter increases the water retention capacity of the soil which is better depicted by the Durner and VGM model.

A few more examples of differences in predicted hydraulic conductivity curves are given Figures 18-21. Different combinations of physical characteristics affect hydraulic conductivities. Although, at the beginning of the simulation, measured hydraulic conductivity was used as initial estimate. Soil texture, landscape location, organic matter content and vegetation cover affects hydraulic conductivity. This hydraulic conductivity is described differently by VGM, Durner's model and DPM, which directly reflects on the assumptions on which these models are developed. At various locations higher hydraulic conductivity is observed as higher drainage rate is observed in fractures (if present). Variation in hydraulic conductivity is observed primarily because of soil texture (grain size and grain size distribution), soil structure (porosity, pore size distribution, geometry and shape of pores and tortuosity). Landscape position (topography), organic matter content and vegetation cover tends to change soil structure and thereby affecting hydraulic conductivity within the watershed.

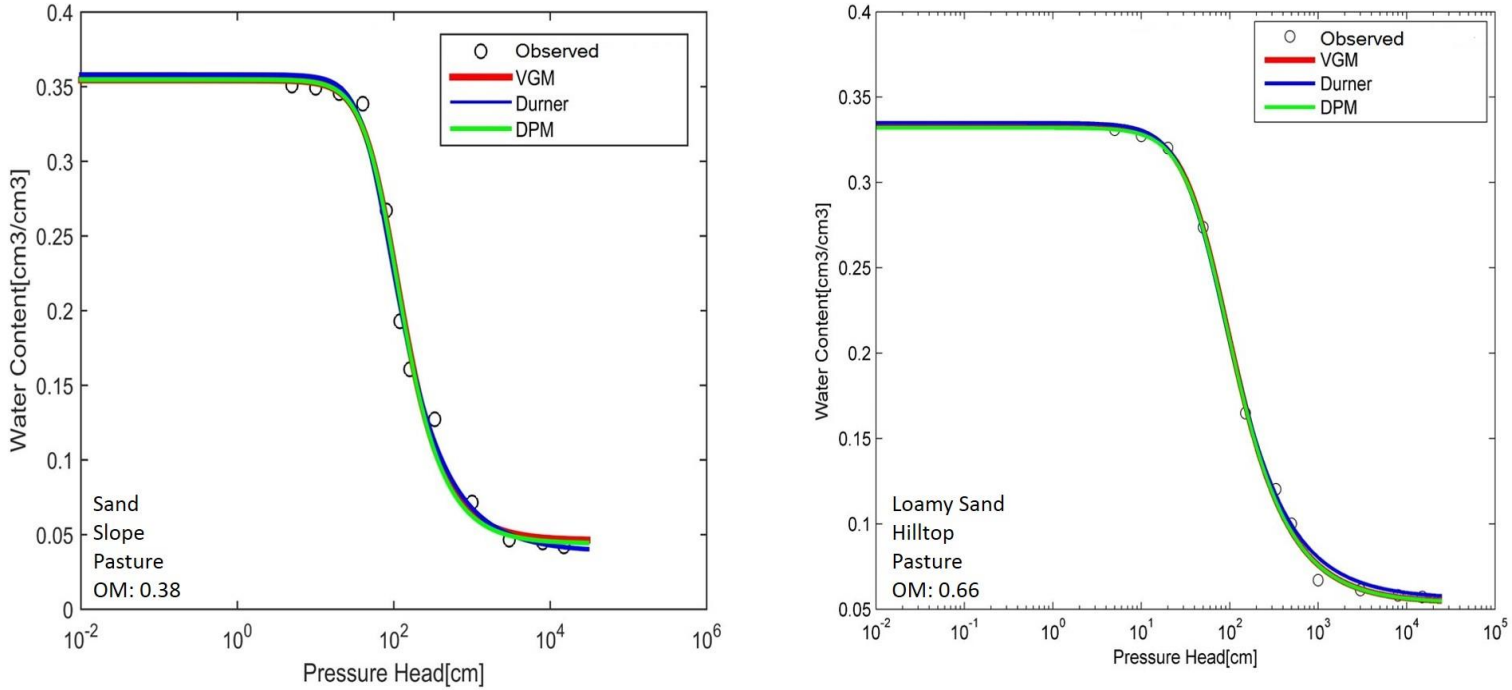

Figure 14: Observed and simulated retention curve of sand and loamy sand type are shown. The data is fitted using VGM, Durner and DPM models.

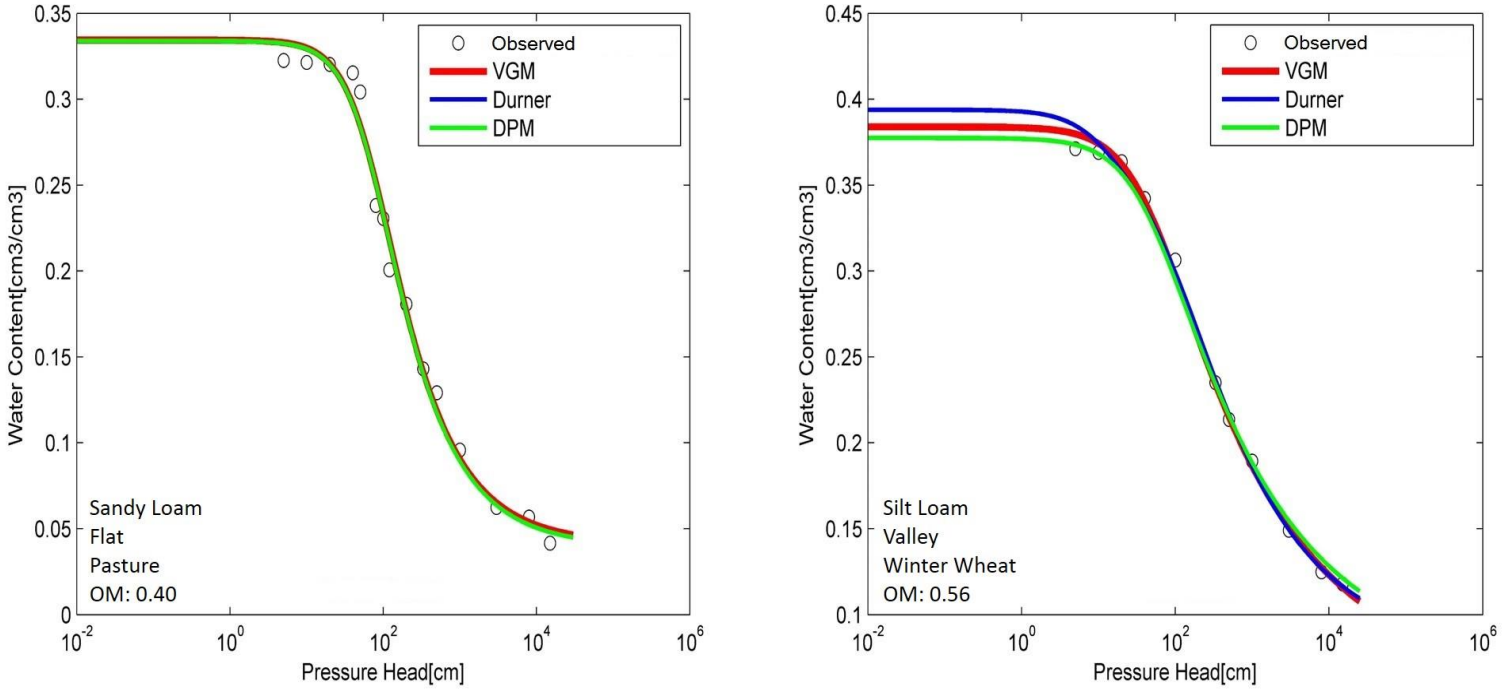

Figure 15: Observed and simulated retention curve of sandy loam and silt loam type are shown. The data is fitted using VGM, Durner and DPM models.

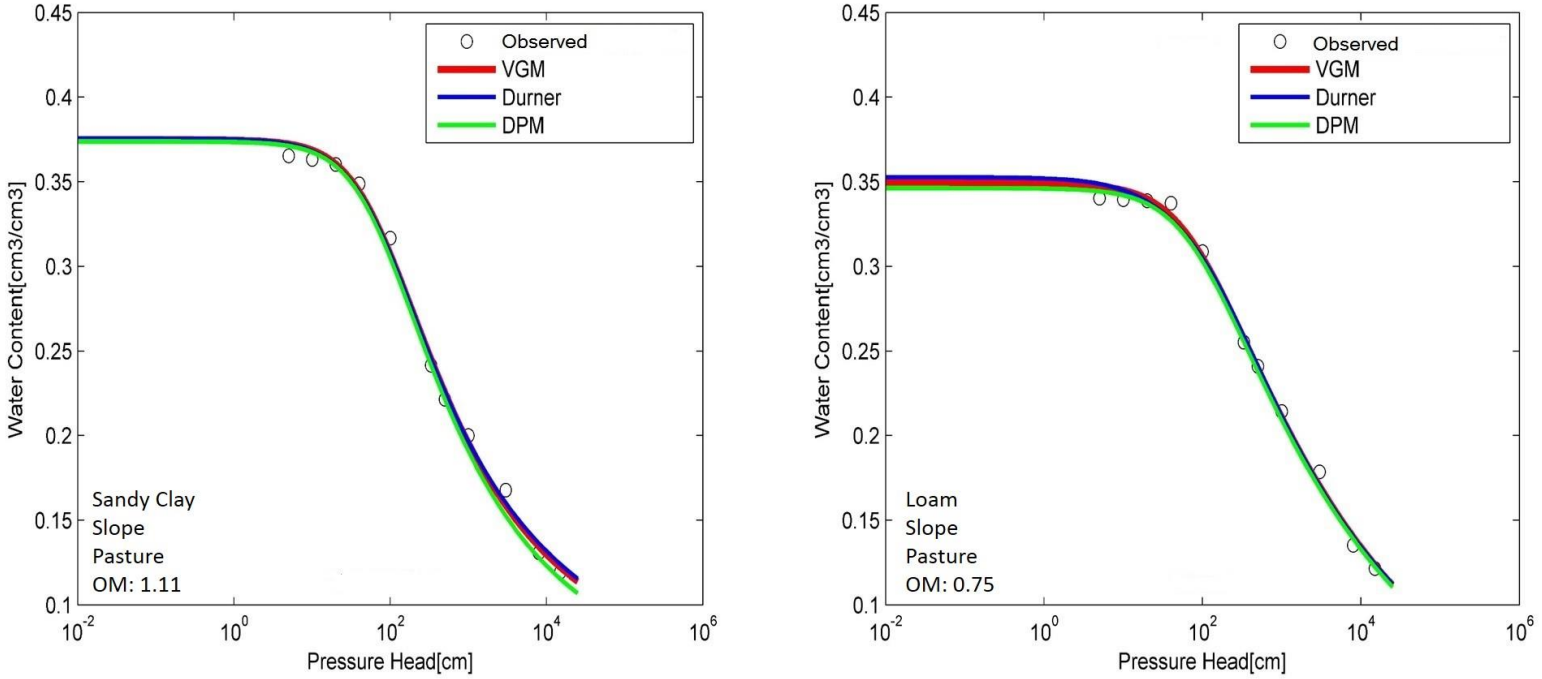

Figure 16: Observed and simulated retention curve of sandy clay and loam type are shown. The data is fitted using VGM, Durner and DPM models. On left, the soil sample was collected with rolling topography, whereas on right the soil sample was collected from flat land.

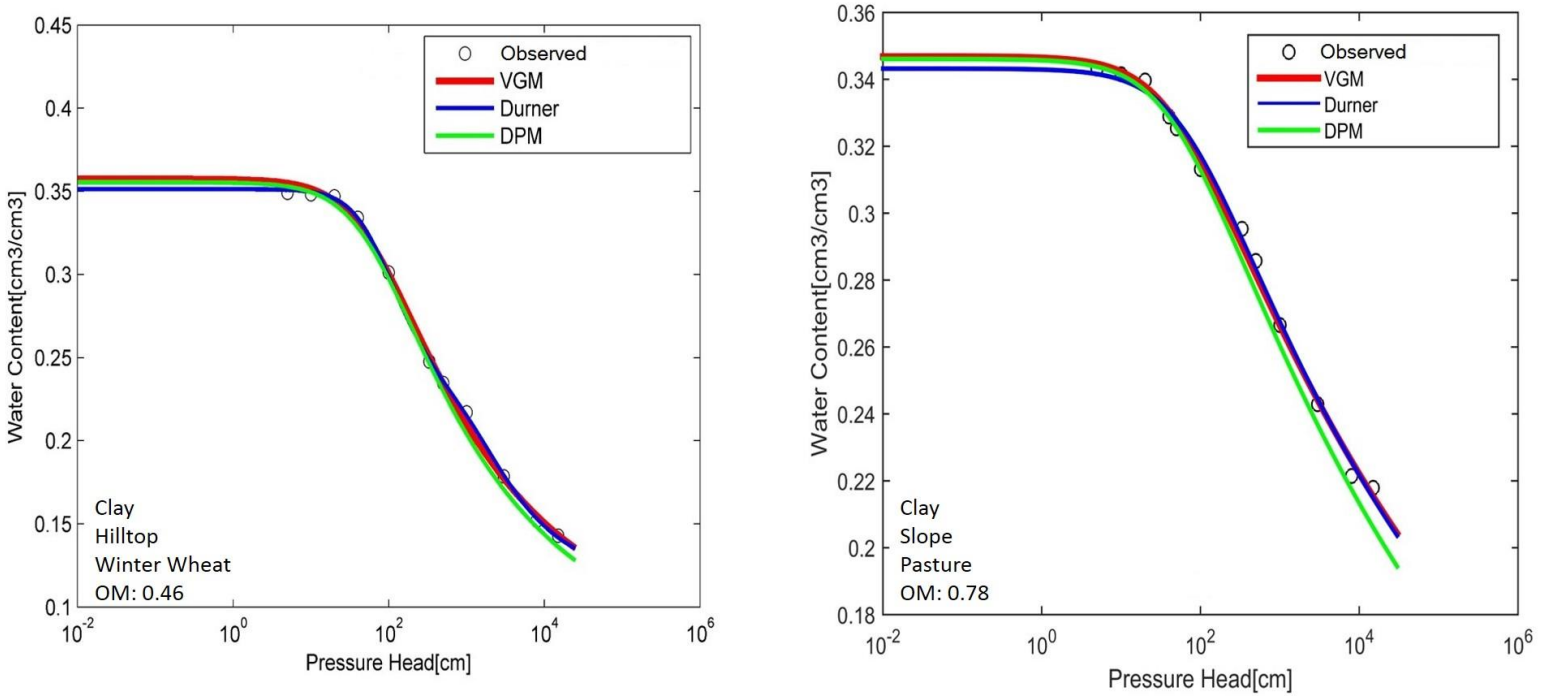

Figure 17: Observed and fitted retention curves for Clay. The data is fitted using VGM, Durner and DPM models. With different topography and organic content we can see how different models vary in fitting.

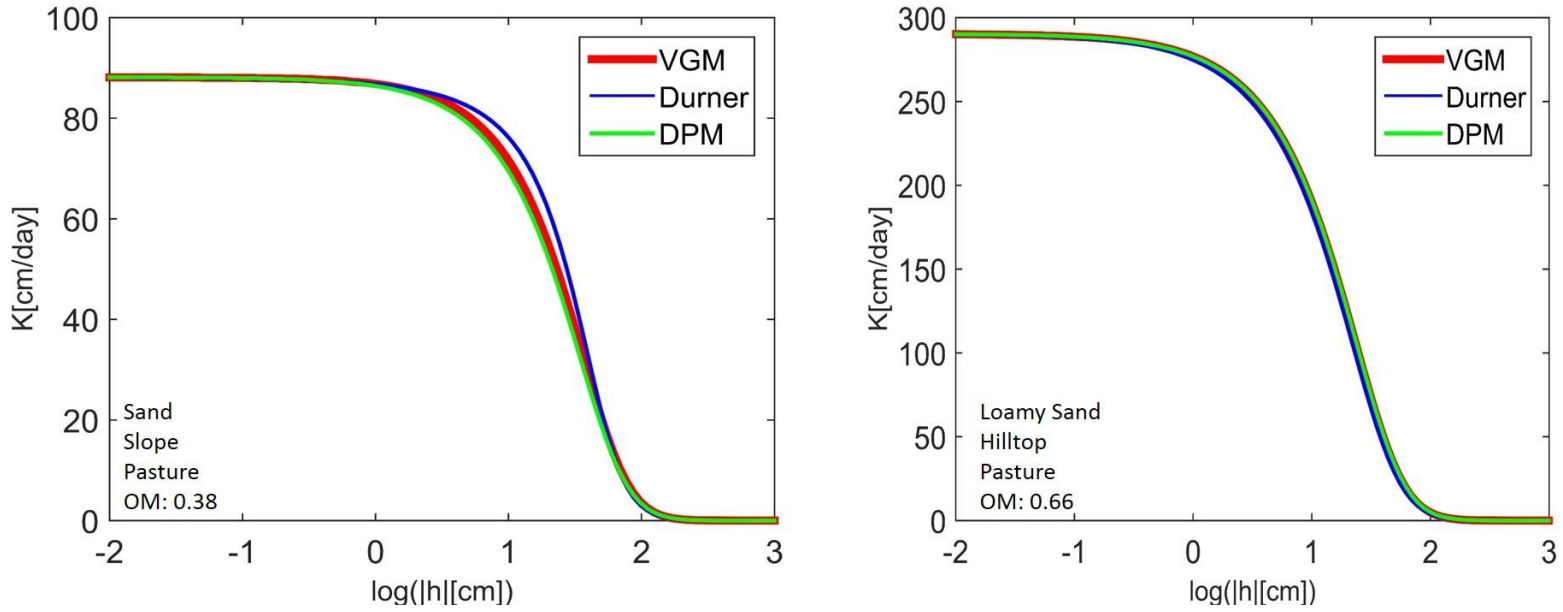

Figure 18: Fitted unsaturated hydraulic conductivity of Sand and Loamy Sand. The data is fitted using VGM, Durner and DPM models.

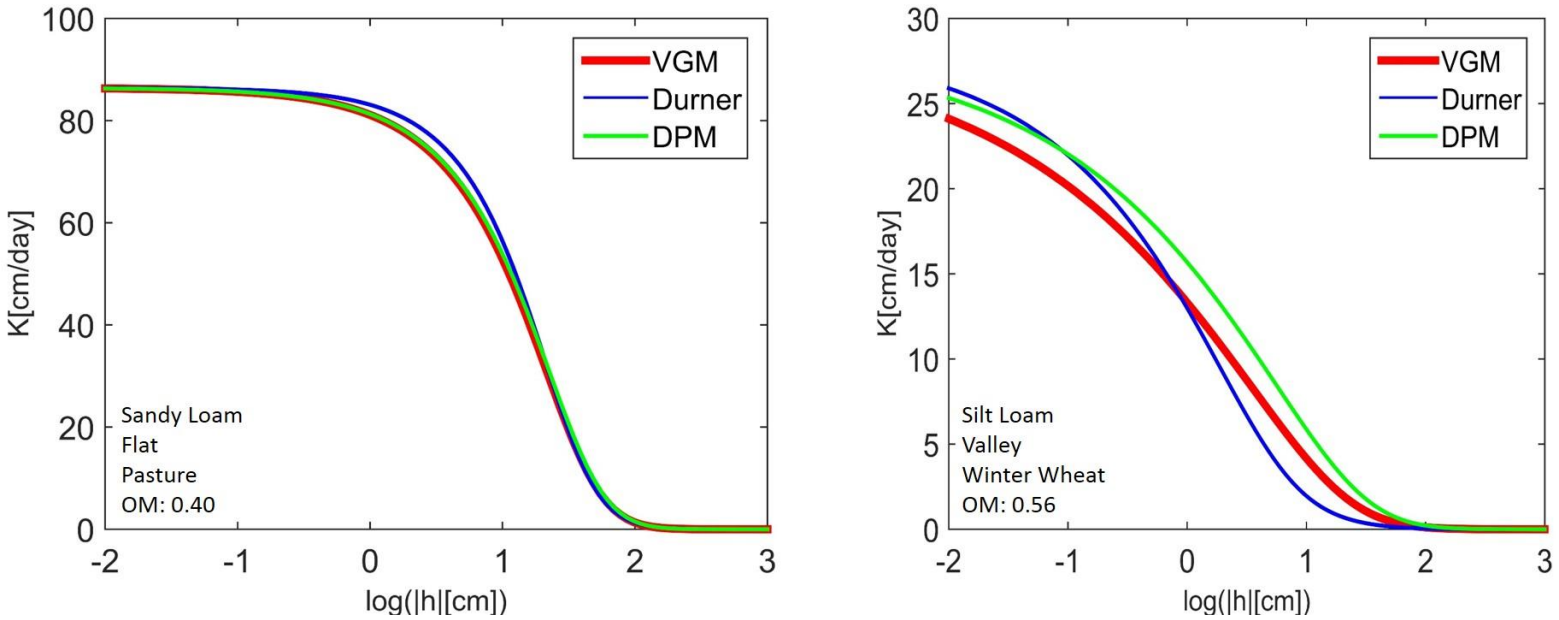

Figure 19: Fitted unsaturated hydraulic conductivity of Sandy Loam and Silt Loam using VGM, Durner and DPM models.

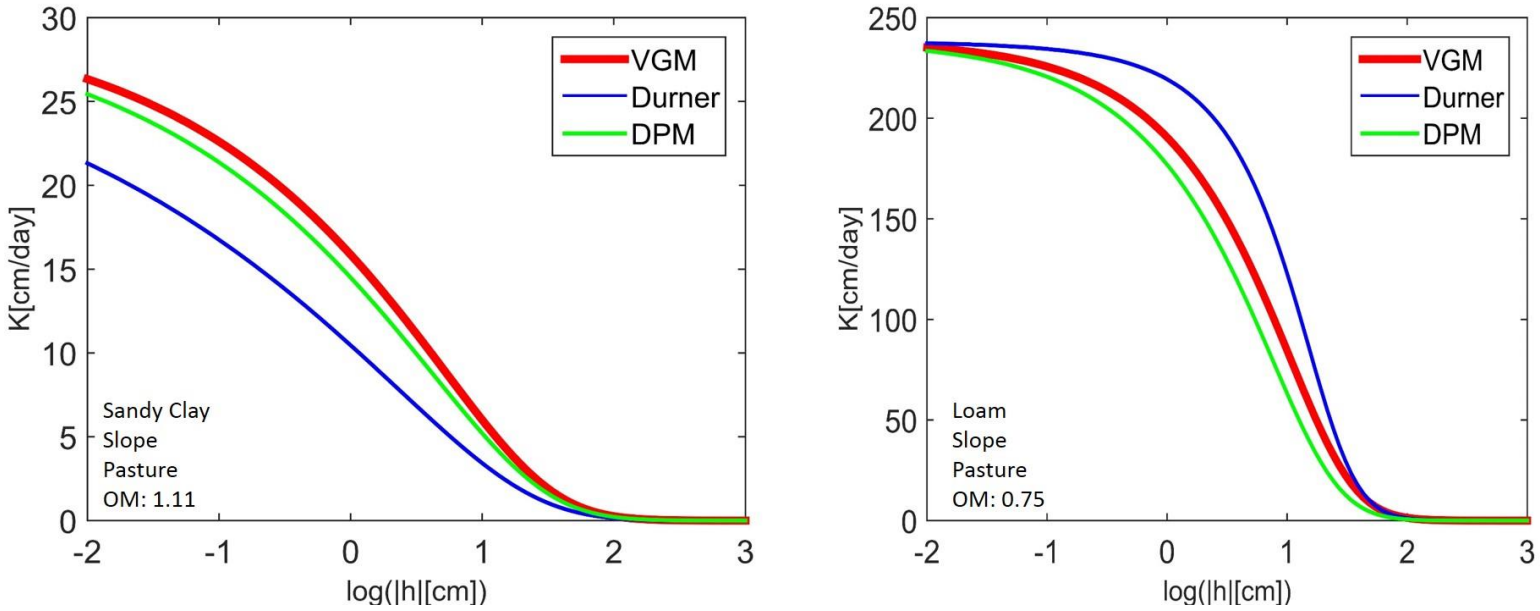

Figure 20: Fitted unsaturated hydraulic conductivity of Sandy Clay and Loam using VGM, Durner and DPM models.

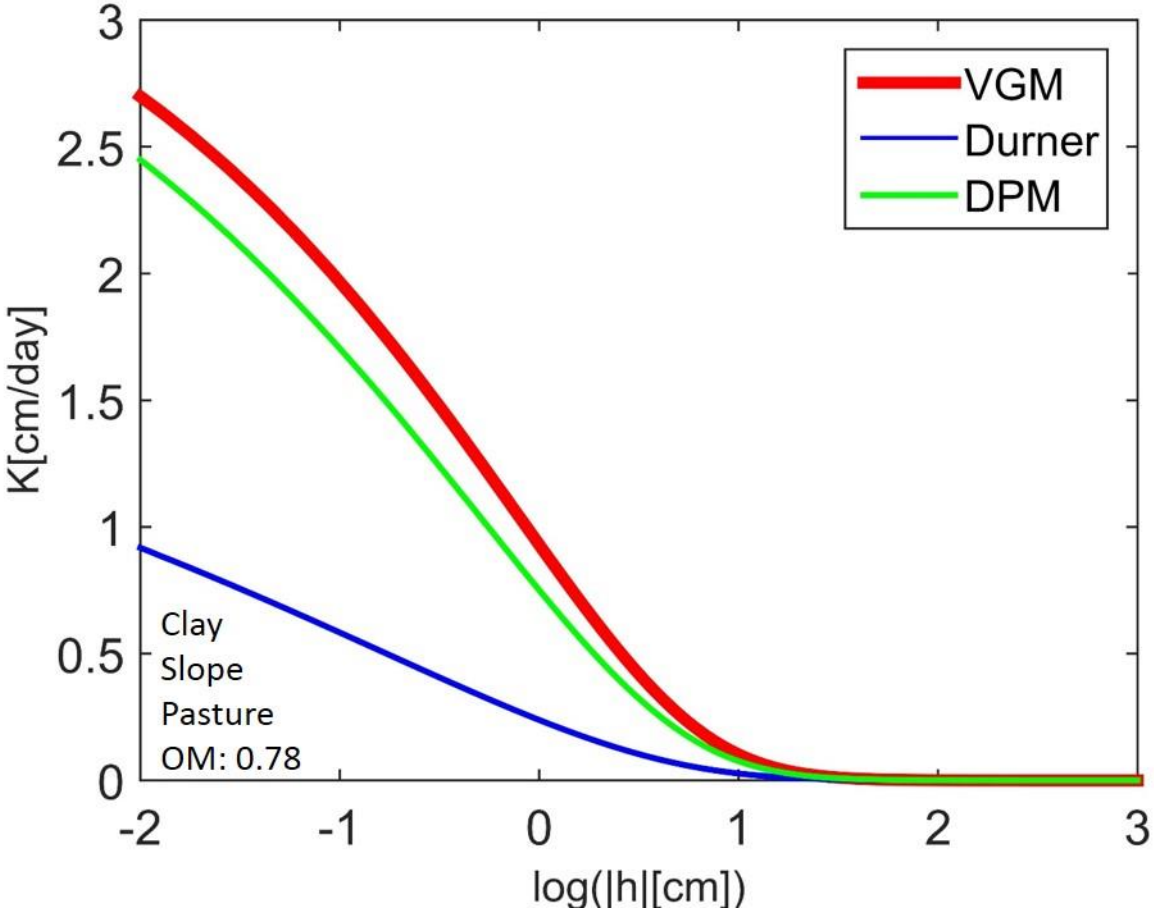

Figure 21: Fitted unsaturated hydraulic conductivity of Clay using VGM, Durner and DPM models.

2.5.3 Forward Modeling

We used calculated SHPs to predict soil moisture dynamics at various watershed locations for a period of time (March 1, 1997-Nov 01, 1997). Since soil samples from different locations differ in soil texture, topography, vegetation cover and organic matter, variability in soil moisture dynamics based on the location (landscape position) of soil sample was observed. We used the three soil water flow models (VGM, Durner and DPM) to predict soil moisture and compared the estimated soil moisture with L-band passive microwave ESTAR instrument during SGP97 field campaign. ESTAR measures (800 m x 800 m) pixel average daily surface (0-5cm) soil moisture content. More elaborate details about remote sensing soil moisture measurement can be found elsewhere [*Mohanty et al.,* 2000; *Njoku and Entekhabi,* 1996; *Schmugge,* 1998]. The ESTAR pixels that were pre-determined as time stable pixels [*Joshi et al*., 2011] were used to validate the forward modeling results. The non-time stable pixels were classified as wet or dry pixels and the soil water flow model that compared best with the ESTAR pixel for each scenario under different heterogeneity conditions was determined. The predicted soil moisture values are also validated with soil moisture values with theta probe hand held sensors which were collected during the SGP97 campaign at various field sites (LW03, LW13 and LW21). The fields are approximately 800 m x 800 m, which is same as the resolution of airbone remote sensing footprint (ESTAR). The volumetric soil moisture in the 0-6cm surface soil layer was measured daily at 49 sampling points, in a regular 7 x 7 square grid with 100 m spacing. To present accurate results, we did not calibrate the forward modeling simulations and therefore are also

compared with soil moisture values calculated using hand held sensors. At many instances, model performance can be improved by qualitative and quantitative measures but in our case, since we used continuum scale models, we relied on absolute soil water content values for validation with ESTAR air borne observations. Since soil water flow models were not calibrated, we selected models based on unbiased results.

Different combinations of soil texture, topography, vegetation and organic content greatly influence the vertical and lateral transmission of water and therefore affect soil hydraulic properties. We have used different topographical conditions in our study (hilltop, valley and slope) and through this we have observed that variations in slope, aspect, curvature and relative elevation affect soil moisture near land surface (0-5cm). Topography can be described by three separate parameters: slope, aspect and location on the slope. Slope influences both infiltration and runoff. Steep slope are likely to be drier than flat areas due to lower infiltration and higher runoff rates. Aspect influences the evapotranspiration within an area and thus, the soil moisture redistribution. Location on the slope affects soil depth. Soils at valley bottoms typically have finer texture and greater depth than that at hilltop. Water routing processes differ with vegetation and with landscape location thereby affecting soil moisture content across the watershed. Due to runoff, organic carbon flows along with water from hill-top to valley through the slopes. Soil organic carbon alters water retention capacity and hydraulic properties. In our study, organic matter content greater than 1% is considered as high, whereas less than 1% is considered low. Land cover which is determined by vegetation is also critical for understanding the soil moisture regimes as it affects

infiltration, runoff and evapotranspiration. Dense root network leads to macropore formation and change in soil organic carbon.

In Figure 22, soil sample from a sandy loam soil, flat topography with thick grass and organic carbon matter >1% is used. This soil sample corresponds to a wet ESTAR pixel [*Joshi et al.*, 2011]. We observed that the Durner and VGM underestimated the soil moisture as compared to the ESTAR observation. On the other hand, predictions using the DPM model were able to capture the soil moisture better. These differences in predicted soil moisture can be attributed to the landscape position of the soil sample which is located at the hill-top with thick grass and high organic carbon. Since the antecedent moisture conditions are not close to saturation (where the DPM loses water fastest amongst the 3 models), the soil moisture drainage is slower in the DPM models than the other two. Thus, DPM predicts higher soil moisture than the other two models which leads to a better match with the typically wet ESTAR pixel. Figure 23 represents a typically wet ESTAR pixel [*Joshi et al.*, 2011], with silt loam in a pasture, flat topography and low carbon content (<0.5%). The soils in this region lack fractured structure and combined with low carbon content to decreases its soil water retention, the Durner model was able to predict the best daily soil moisture pattern (Figure 23) as compared to DPM which overestimated soil moisture consistently. In few cases, the VGM model could also capture the soil moisture dynamics for this pixel. Figure 24 represents a dry, homogenous soil (sand), flat topography landscape location in pasture with low carbon content. That pixel showed mixed results. VGM was able to predict daily soil moisture but at slope with higher organic content DPM was able predict better

than VGM and Durner, as seen in Figure 24. Figure 25 represents a dry pixel with vegetation density (>90%) on slope, clayey soil and organic carbon less than 1%. Previous studies show that under clayey conditions (which typically indicate significant soil structure), DPM better captures soil moisture dynamics as opposed to Durner and VGM [*Jarvis*, 2007]. DPM overestimates soil moisture than actual soil water content, most likely due to higher drainage rate at a slope in soil matrix of the clayey soil, which cannot be accounted for by the DPM. The alterations to the soil matrix are caused as a result of the presence of organic matter and vegetation. We observed that VGM was the closest match to the dry ESTAR pixel. This analysis reveals that under heterogeneous field conditions, different combinations of heterogeneity factors like organic matter, vegetation, topography act together to alter the pore structure of the soil and hence influence the water flow regime. This causes variation in the expected performance of models suited for various soil types (like DPM for structured clay soils) under varying heterogeneity conditions.

Based on these observations, a scheme for selecting the best model under different landscape conditions was developed (Table 4). Based on different physical characteristics of a location this modeling scheme can be useful in the estimation of soil water content. These soil samples are further classified as time stable (TS), wet and dry, with reference to the location of the soil sample in the watershed. The highest permissible RMSE in this scheme was set to 4%, which is the permissible error for ESTAR air borne observations [*Drusch et al.*, 2004].

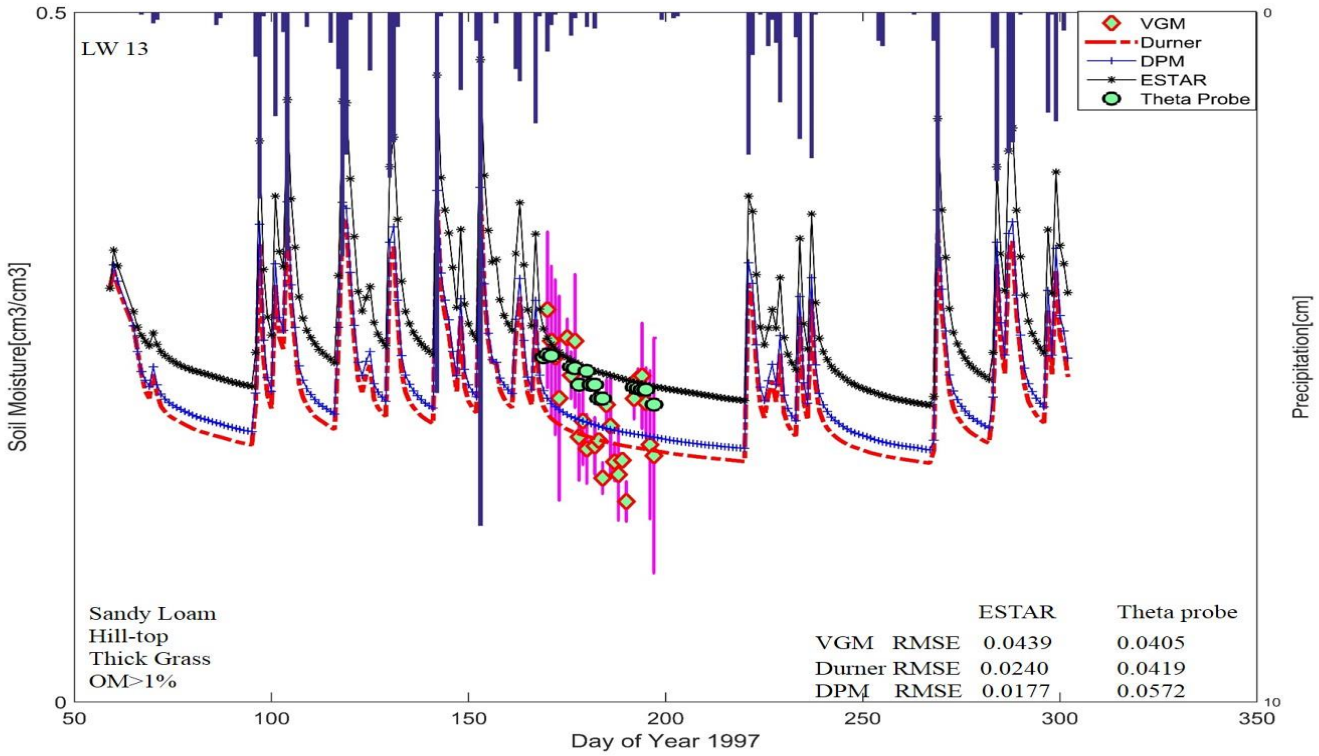

Figure 22: Simulated soil moisture from March through November 1997. VGM, Durner and DPM predict differently under different physical conditions.

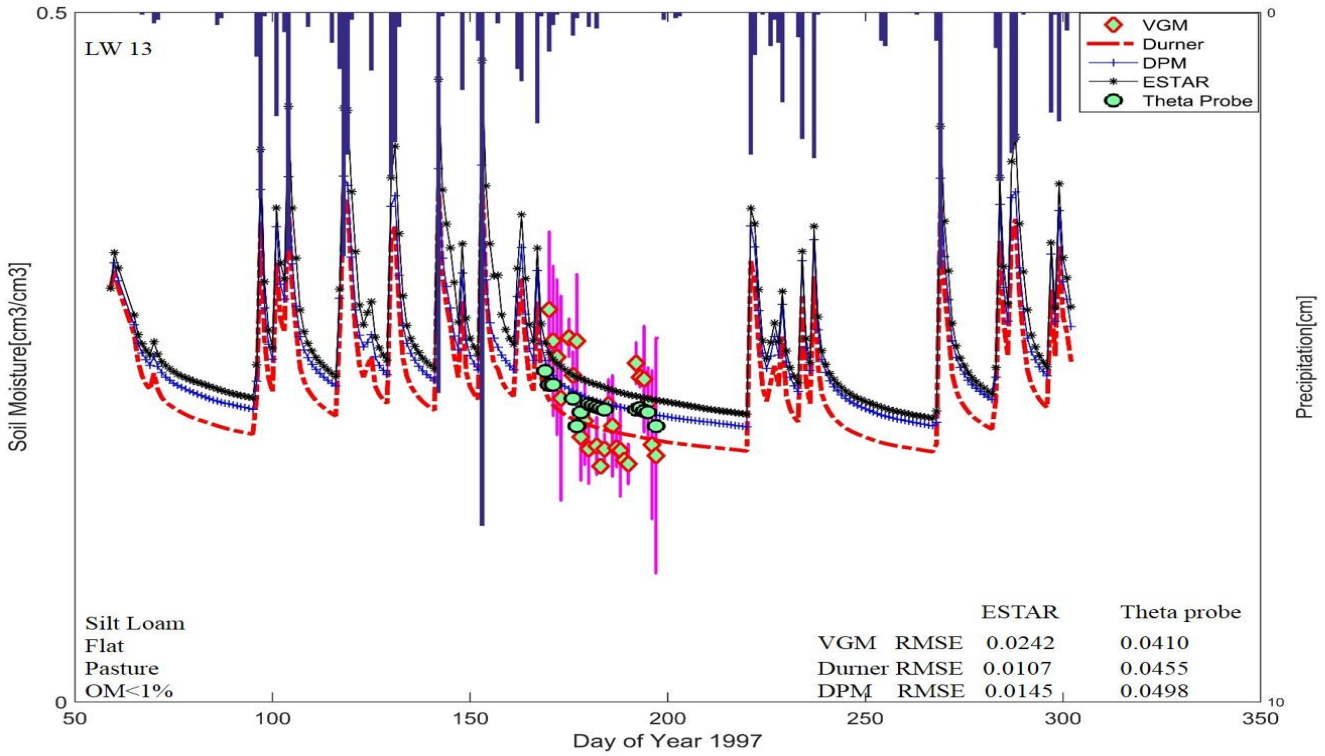

Figure 23: Simulated soil moisture prediction from March through November 1997. VGM, Durner and DPM predict differently under different physical conditions.

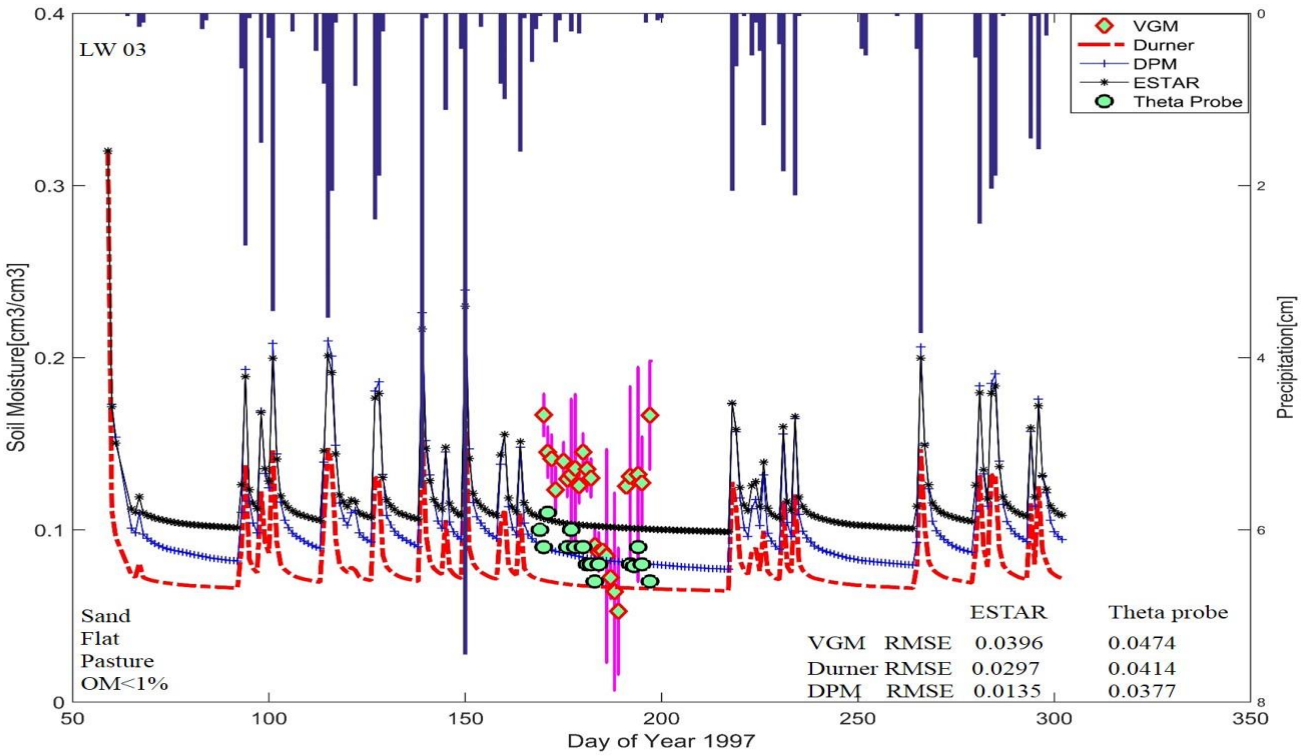

Figure 24: Simulated soil moisture prediction from March through November 1997. VGM, Durner and DPM predict differently under different physical conditions.

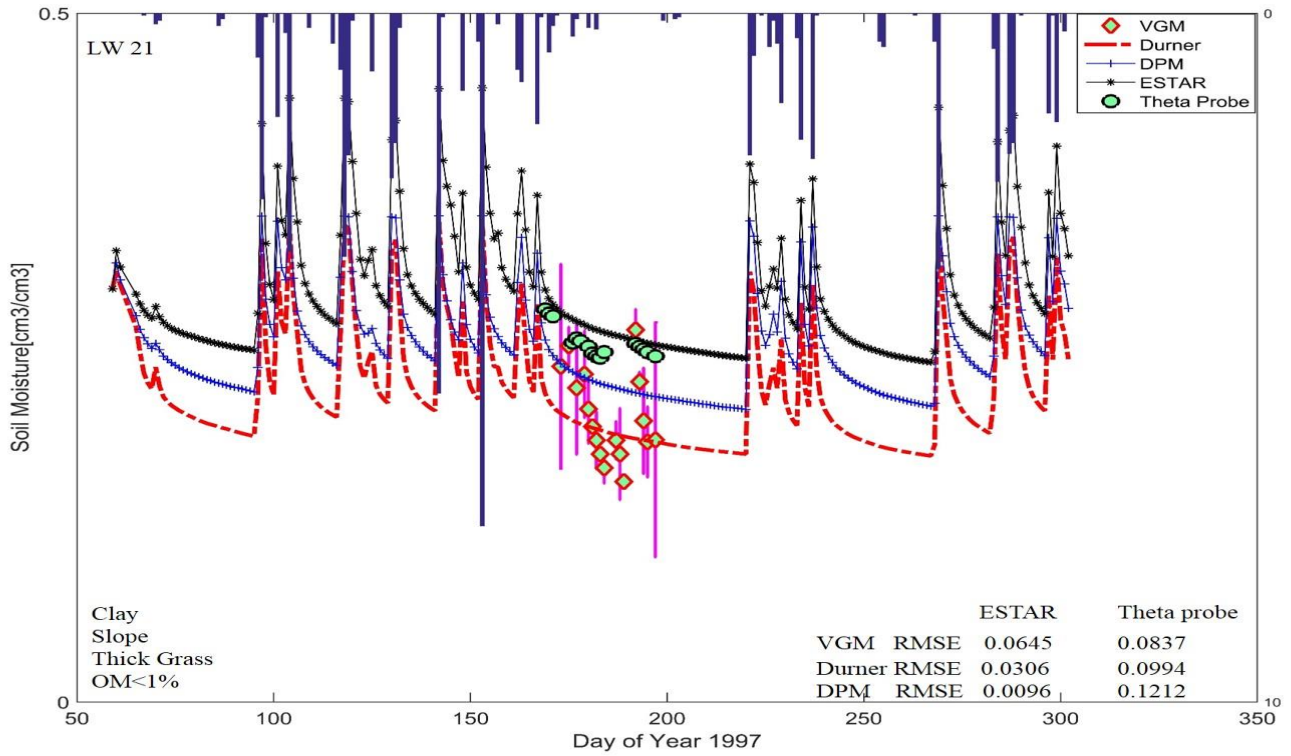

Figure 25: Simulated soil moisture prediction from March through November 1997. VGM, Durner and DPM predict differently under different physical conditions.

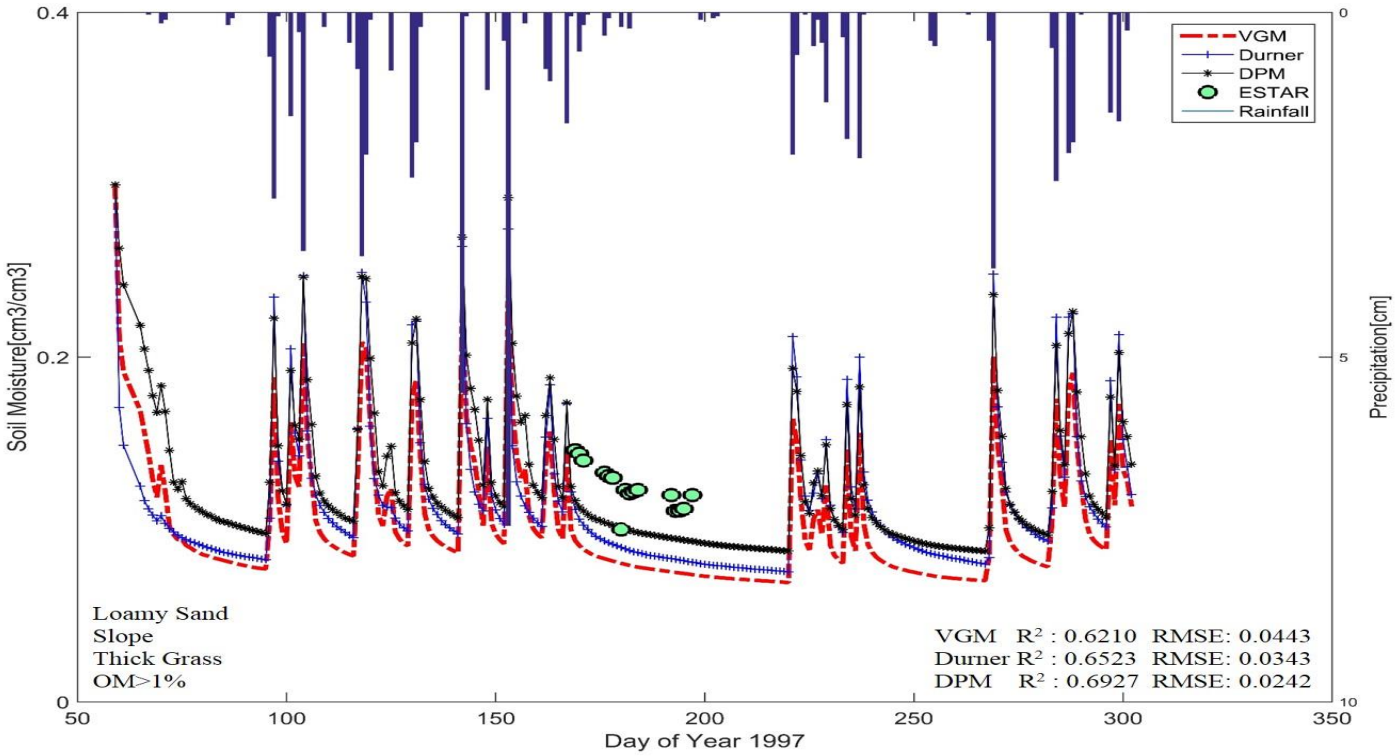

Figure 26: Simulated soil moisture prediction from March through November 1997. VGM, Durner and DPM predict differently under different physical conditions.

Table 4: Soil moisture prediction scheme. This helps a user to determine which continuum scale model is appropriate under certain set of conditions.

Sample ID	Soil type	Soil Depth	Landscape Position	Vegetation Type	Organic Matter (%)	Model Preferred	Type of Location
5	L	0-30	Valley	Grass	0.96	Durner	Wet
7	L	60-90	Valley	Grass	0.38	DPM	Wet
8	L	70-75	Valley	Grass	0.38	VGM	Wet
12	LS	3-9	Hilltop	Pasture	0.4	DPM	TS
13	SL	3-9	Hilltop	Pasture	0.15	VGM	Dry
15	S	3-9	Slope	Pasture	0.3	VGM	Wet
16	S	3-9	Slope	Pasture	0.38	VGM	Dry
17	SL	6-12	Bottom	Pasture	0.46	DPM	TS
21	SL	0-30	Mid-slope	Pasture	0.29	DPM	Wet
23	SL	53-59	-	-	0.25	Durner	Dry
24	LS	3-9	Top	Pasture	0.66	DPM	Dry
26	SCL	13-18	-	-	0.42	-	Dry
29	LS	3-9	Mid-slope	Pasture	0.72	Durner	Wet
32	SL	3-9	Mid-slope	Grass	0.5	DPM	TS
35	SCL	19-25	Top of crest	Pasture	0.73	DPM	Wet
36	SCL	40-46	Top of crest	Pasture	0.44	-	Wet
37	SCL	60-90	Top of crest	Pasture	0.16	DPM	Wet
38	SL	3-9	Mid-slope	Grass	0.37	DPM	Dry
39	SL	3-9	Mid-slope	Grass	0.49	Durner	Dry
41	S	23-29	Bottom	Grass	0.13	VGM	Dry
54	L	38-44	Flat Field	Grass	0.41	Durner	Dry
55	SiL	73-79	Flat Field	Grass	0.3	DPM	Dry
58	SiL	3-9	Bottom	Pasture	1.51	Durner	TS
67	SCL	3-9	Mid-slope	Pasture	1.11	-	Wet
69	LS	3-9	Flat Land	Pasture	0.84	DPM	Wet
70	S	3-9	Mid-slope	Pasture	0.27	VGM	Dry
71	S	3-9	Near Top	Pasture	0.26	DPM	Wet
73	LS	3-9	Slope	Pasture	0.47	DPM	Wet
74	LS	3-9	Top of Ridge	Pasture	0.61	DPM	Wet
75	S	3-9	Hilltop	Pasture	0.36	VGM	Dry
78	SL	20-40	Flat Field	Pasture	0.4	DPM	Dry
79	SL	40-60	Flat	Pasture	0.4	DPM	Wet
88	CL	28-34	Valley	Pasture	1.74	DPM	Dry
100	SiCL	48-54	Flat Field	Winter Wheat	0.71	Durner	Dry
101	CL	73-79	Flat Field	Winter Wheat	-	-	Dry
102	CL	93-99	Hilltop	Winter Wheat	-	-	Wet
104	SiCL	53-59	Flat Field	Pasture	0.62	Durner	Dry
105	SiC	83-89	Flat Field	Pasture	0.38	DPM	Dry
108	SiL	3-9	Valley	Winter Wheat	0.66	DPM	TS
109	SiL	33-39	Valley	Winter Wheat	1.56	Durner	Dry

Table 4 Continued

Sample ID	Soil type	Soil Depth	Landscape Position	Vegetation Type	Organic Matter (%)	Model Preferred	Type of Location
110	CL	53-59	Flat Field	Winter Wheat	0.67	DPM	Wet
111	CL	76-82	Flat Field	Winter Wheat	0	DPM	Dry
113	L	3-9	Hilltop	-	0.37	DPM	Wet
114	SiL	3-9	Hilltop	Pasture	1.76	VGM	TS
115	CL	3-9	Slope	Pasture	0.78	-	Dry
116	L	3-9	Slope	Pasture	0.75	DPM	Wet
151	SiC	3-9	Valley	-	-	-	Dry
152	SiCL	3-9	Valley	-	-	-	Wet
153	SiCL	3-9	Valley	-	-	-	Wet

2.5.4 Validation with Time Stable Locations

The simulated soil moisture predictions were validated using soil moisture at TS locations similar to locations *Joshi et al.* [2011]. These TS locations from *Joshi et al.* [2011] are shown in the Figure 27 (used with permission). Using our soil water flow model prediction scheme, we selected the appropriate model and compared soil moisture values for TS locations. The details of physical controls of these locations are given in Table 5 and the results are shown in Figure 28.

Table 5: Details of Time Stable locations are presented with their soil texture, topography, vegetation and organic matter. The preferred model is used to predict the soil moisture.

Sample ID	Soil Texture	Topography	Vegetation	Organic Matter %	Preferred Model	R^2	RMSE
Sample 58	Silt Loam	Flat	Mixed Grass	1.51	Durner	0.68	0.02
Sample 114	Silt Loam	Slope	Wheat	0.46	VGM	0.83	0.01
Sample 12	Loamy Sand	Rolling	Pasture	0.37	DPM	0.92	0.01
Sample 17	Sandy Loam	Rolling	Pasture	1.76	DPM	0.84	0.004

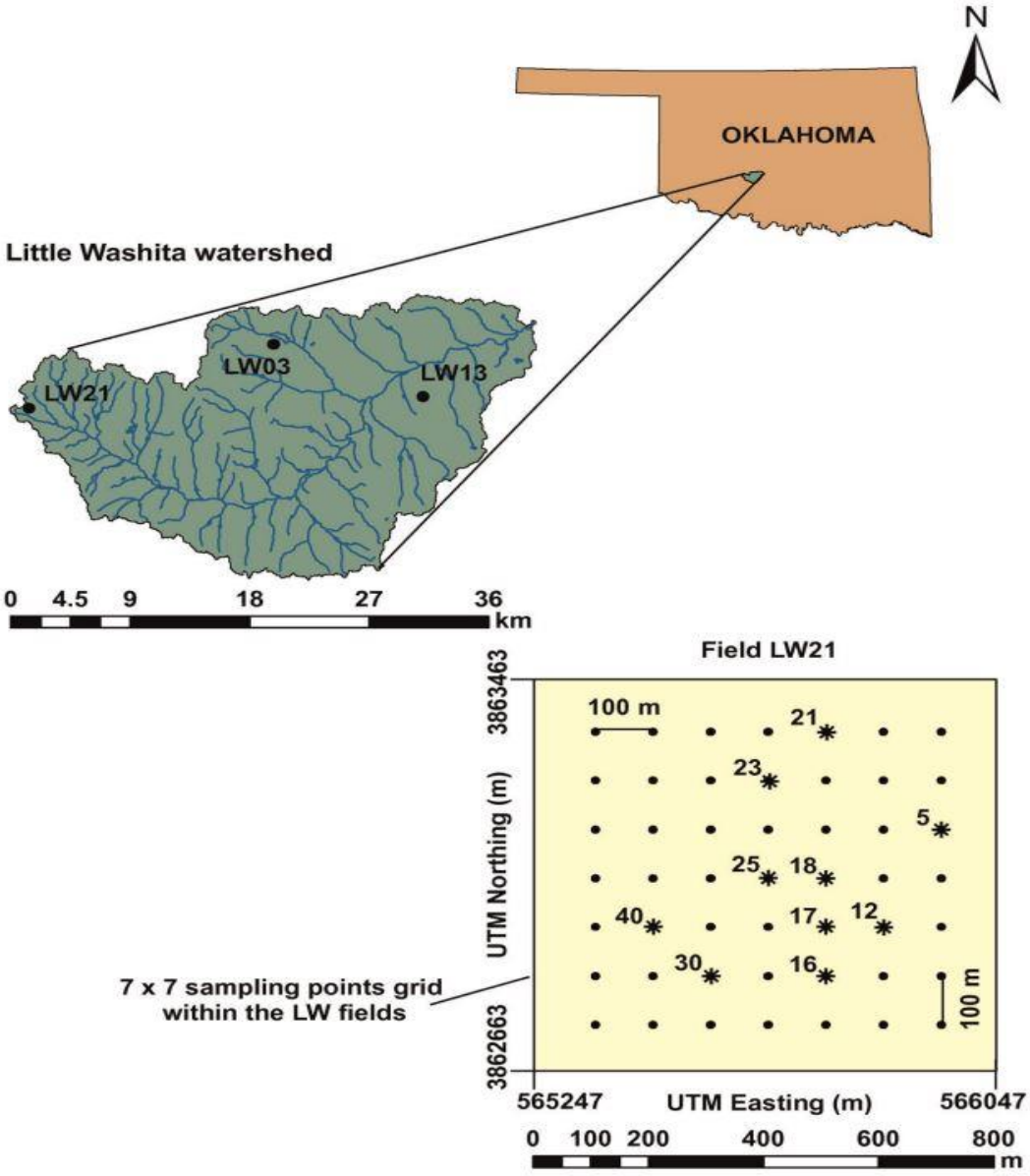

Figure 27: Sampling points grid within Little Washita, watershed, Oklahoma during the SGP97 campaign as presented in Joshi et al. [2011]. Time stable locations were selected from results and validated with our modeling results.

The detailed validation results for four time stable locations (sample 58, sample 114, sample 12 and sample 17) and their respective R^2 and RMSE values are shown in Figure 28. The error bars reflect the standard deviation of the modeled soil moisture for the duration of the remote sensing data collection efforts. With the help of this validation we can say that the soil water flow model scheme to predict soil moisture can be used elsewhere and is transferable, provided the details of the physical controls are available.

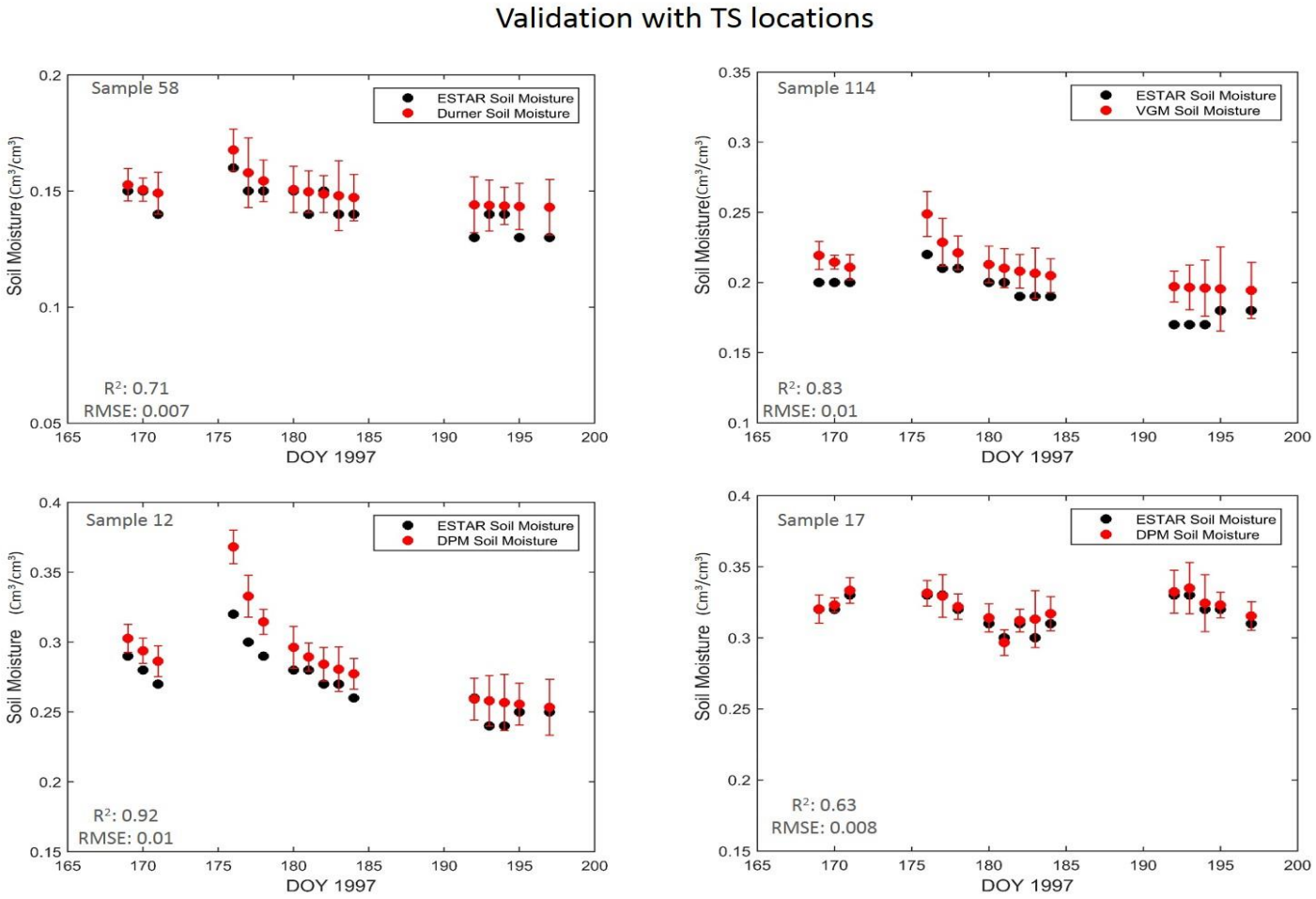

Figure 28: Selected soil water flow model using prediction scheme is used to calculate soil moisture and have been validated with ESTAR soil moisture values. The modeled soil moisture shows error bars based on standard deviation values.

CHAPTER III

CONCLUSIONS

Three models (VGM, Durner's and DPM) were used to calculate SHPs using inverse modeling at various locations within the Little Washita watershed. Soil sample collected were used to analyze the SHPs and preferential flow. Water flow is described differently in porous media by different continuum scale models, as a result of differences in pore size distribution and pore connectivity in structured soils. Various non-equilibrium effects such as entrapment of water, pore water blockage and air entrapment were noticed while calculating soil hydraulic properties using inverse modeling. Since, each soil water flow model is conceptually different; we noticed variations in the calculated soil hydraulic parameters. These variations were observed in hydraulic conductivity thereby affecting soil water retention.

The calculated soil hydraulic parameters were used to predict soil moisture for a period of eight months using three continuum scale models. We observed that within a watershed factors such as soil texture, topography, vegetation cover and organic matter content can significantly contribute towards soil water content. Different combinations of soil texture, topography, vegetation and organic content greatly influenced the calculation of soil hydraulic properties and soil moisture prediction. For most of the combinations, dual porosity model was able to capture the micro and macro heterogeneities better than Durner's and single porosity model. But factors such as landscape position, organic matter and vegetation have significantly contributed in predicting soil moisture. Variability in predicted soil moisture using different flow

models was higher for coarse soils with varying contents of organic matter i.e. higher estimation of soil moisture was observed with higher organic matter content. Using this knowledge we developed a scheme for selection of model, based on the physical properties of the landscape position or location. This technique will be useful for calculating the soil water content for places for which remotely sensed data or ground sampling stations are not available. Because this model prediction scheme has been validated with time stable locations in Little Washita watershed, we expect this scheme to be transferrable to other locations, provided the physical characteristics are known.

REFERENCES

Allen, P. B. and J. W. Naney (1991), Hydrology of the Little Washita river watershed, Oklahoma: Data and analyses, *ARS-US Department of Agriculture, Agricultural Research Service (USA)*.

Assouline, S. and D. Or (2013), Conceptual and parametric representation of soil hydraulic properties: A review, *Vadose Zone Journal*, *12*(4).

Beke, G. and M. MacCormick (1985), Predicting volumetric water retentions for subsoil materials from Colchester County, Nova Scotia, *Can. J. Soil Sci.*, *65*(1), 233-236.

Beven, K. (1991), Modeling preferential flow: an uncertain future, *Preferential Flow*, 1-11.

Castillo, V., A. Gomez-Plaza, and M. Martınez-Mena (2003), The role of antecedent soil water content in the runoff response of semiarid catchments: a simulation approach, *Journal of Hydrology*, *284*(1), 114-130.

Clausnitzer, V. and J. Hopmans (1995), Non-linear parameter estimation: LM_OPT, *General-purpose optimization code based on the Levenberg–Marquardt algorithm.Land, Air and Water Resources Paper No. 100032*, University of California, Davis, CA.

Das, Narendra N. (2005). Soil moisture modeling and scaling using passive microwave remote sensing. Master's thesis, Texas A&M University. Texas A&M University. Available electronically from http://hdl.handle.net/1969.1/4881.

Diamantopoulos, E., S. Iden, and W. Durner (2012), Inverse modeling of dynamic nonequilibrium in water flow with an effective approach, *Water Resour. Res.*, *48*(3).

Diamantopoulos, E. and W. Durner (2012), Dynamic nonequilibrium of water flow in porous media: A review, *Vadose Zone Journal*, *11*(3).

Diks, C. G. and J. A. Vrugt (2010), Comparison of point forecast accuracy of model averaging methods in hydrologic applications, *Stochastic Environmental Research and Risk Assessment*, *24*(6), 809-820.

Drusch, M., E. F. Wood, H. Gao, and A. Thiele (2004), Soil moisture retrieval during the Southern Great Plains Hydrology Experiment 1999: A comparison between experimental remote sensing data and operational products, *Water Resour. Res.*, *40*(2).

Durner, W. (1994), Hydraulic conductivity estimation for soils with heterogeneous pore structure, *Water Resour. Res., 30*(2), 211-223.

Durner, W., E. Priesack, H. Vogel, and T. Zurmühl (1999a), Determination of parameters for flexible hydraulic functions by inverse modeling, *Characterization and measurement of the hydraulic properties of unsaturated porous media.University of California, Riverside, CA*, 817-829.

Durner, W., B. Schultze, and T. Zurmühl (1999b), State-of-the-art in inverse modeling of inflow/outflow experiments, *Characterization and measurement of the hydraulic properties of unsaturated porous media.Univ.of California, Riverside*, 661-681.

Durner, W., B. Schultze, and T. Zurmühl (1999c), State-of-the-art in inverse modeling of inflow/outflow experiments, *Characterization and measurement of the hydraulic properties of unsaturated porous media.Univ.of California, Riverside*, 661-681.

Eching, S. and J. Hopmans (1993), Optimization of hydraulic functions from transient outflow and soil water pressure data, *Soil Sci. Soc. Am. J., 57*(5), 1167-1175.

Eching, S., J. Hopmans, and O. Wendroth (1994), Unsaturated hydraulic conductivity from transient multistep outflow and soil water pressure data, *Soil Sci. Soc. Am. J., 58*(3), 687-695.

Famiglietti, J., J. Devereaux, C. Laymon, T. Tsegaye, P. Houser, T. Jackson, S. Graham, M. Rodell, and P. Van Oevelen (1999), Ground-based investigation of soil moisture variability within remote sensing footprints during the Southern Great Plains 1997 (SGP97) Hydrology Experiment, *Water Resour. Res., 35*(6).

Feyen, J., D. Jacques, A. Timmerman, and J. Vanderborght (1998), Modelling water flow and solute transport in heterogeneous soils: A review of recent approaches, *J. Agric. Eng. Res., 70*(3), 231-256.

Figueras, J. and M. M. Gribb (2009), Design of a user-friendly automated multistep outflow apparatus, *Vadose Zone Journal, 8*(2), 523-529.

Flühler, H., W. Durner, and M. Flury (1996), Lateral solute mixing processes—A key for understanding field-scale transport of water and solutes, *Geoderma, 70*(2), 165-183.

Friedman, S. P. (1999), Dynamic contact angle explanation of flow rate-dependent saturation-pressure relationships during transient liquid flow in unsaturated porous media, *J. Adhes. Sci. Technol., 13*(12), 1495-1518.

Gaur, N. and B. P. Mohanty (2013), Evolution of physical controls for soil moisture in humid and subhumid watersheds, *Water Resour. Res., 49*(3), 1244-1258.

Gee, G., C. Kincaid, R. Lenhard, and C. Simmons (1991), Recent studies of flow and transport in the vadose zone, *Rev. Geophys., 29*, 227-239.

Gerke, H. and M. v. Genuchten (1993), A dual- porosity model for simulating the preferential movement of water and solutes in structured porous media, *Water Resour. Res., 29*(2), 305-319.

Hanson, J. D., K. Rojas, and M. J. Shaffer (1999), Calibrating the root zone water quality model, *Agron. J., 91*(2), 171-177.

Hassanizadeh, S. M., M. A. Celia, and H. K. Dahle (2002), Dynamic effect in the capillary pressure–saturation relationship and its impacts on unsaturated flow, *Vadose Zone Journal, 1*(1), 38-57.

Hollis, J., R. Jones, and R. Palmer (1977), The effects of organic matter and particle size on the water-retention properties of some soils in the West Midlands of England, *Geoderma, 17*(3), 225-238.

Hopmans, J., J. Šimůnek, N. Romano, and W. Durner (2002), 3.6. 2. Inverse Methods, *Methods of Soil Analysis: Part 4 Physical Methods*(methodsofsoilan4), 963-1008.

Jacobs, J. M., B. P. Mohanty, E. Hsu, and D. Miller (2004), SMEX02: Field scale variability, time stability and similarity of soil moisture, *Remote Sens. Environ., 92*(4), 436-446.

Jarvis, N. (1998), Modeling the impact of preferential flow on nonpoint source pollution, *Physical Nonequilibrium in Soils: Modeling and Application, Ann Arbor Press, Chelsea, MI*, 195-221.

Jarvis, N. (2007), A review of non- equilibrium water flow and solute transport in soil macropores: Principles, controlling factors and consequences for water quality, *Eur. J. Soil Sci., 58*(3), 523-546.

Klute, A. and C. Dirksen (1986), Hydraulic conductivity and diffusivity: Laboratory methods, *Methods of Soil Analysis: Part 1—Physical and Mineralogical Methods*(methodsofsoilan1), 687-734.

Köhne, J. M., S. Köhne, and J. Šimůnek (2009), A review of model applications for structured soils: a) Water flow and tracer transport, *J. Contam. Hydrol., 104*(1), 4-35.

Laloy, E., M. Weynants, C. Bielders, M. Vanclooster, and M. Javaux (2010), How efficient are one-dimensional models to reproduce the hydrodynamic behavior of structured soils subjected to multi-step outflow experiments?, *Journal of hydrology, 393*(1), 37-52.

Leij, F. J. (1996), *The UNSODA Unsaturated Soil Hydraulic Database: User's Manual*, vol. 96, National Risk Management Research Laboratory, Office of Research and Development, US Environmental Protection Agency.

Lin, H., K. Mclnnes, L. Wilding, and C. Hallmark (1998), Macroporosity and initial moisture effects on infiltration rates in vertisols and vertic intergrades., *Soil Sci., 163*(1), 2-8.

Messing, I. and N. Jarvis (1990), Seasonal variation in field- saturated hydraulic conductivity in two swelling clay soils in Sweden, *J. Soil Sci., 41*(2), 229-237.

Mirzaei, M. and D. B. Das (2007), Dynamic effects in capillary pressure–saturations relationships for two-phase flow in 3D porous media: Implications of micro-heterogeneities, *Chemical engineering science, 62*(7), 1927-1947.

Mohanty, B. P. and J. Zhu (2007), Effective hydraulic parameters in horizontally and vertically heterogeneous soils for steady-state land-atmosphere interaction, *J. Hydrometeorol., 8*(4), 715-729.

Mohanty, B., P. Shouse, D. Miller, and M. T. van Genuchten (2002), Soil property database: Southern Great Plains 1997 hydrology experiment, *Water Resour. Res., 38*(5), 5-1-5-7.

Mohanty, B. and T. Skaggs (2001), Spatio-temporal evolution and time-stable characteristics of soil moisture within remote sensing footprints with varying soil, slope, and vegetation, *Adv. Water Resour., 24*(9), 1051-1067.

Mohanty, B., T. H. Skaggs, and J. Famiglietti (2000), Analysis and mapping of field-scale soil moisture variability using high- resolution, ground- based data during the Southern Great Plains 1997 (SGP97) Hydrology Experiment, *Water Resour. Res., 36*(4), 1023-1031.

Mualem, Y. (1976), A new model for predicting the hydraulic conductivity of unsaturated porous media, *Water Resour. Res., 12*(3), 513-522.

Nasta, P., T. Kamai, G. B. Chirico, J. W. Hopmans, and N. Romano (2009), Scaling soil water retention functions using particle-size distribution, *Journal of hydrology, 374*(3), 223-234.

Nemes, A., M. Schaap, F. Leij, and J. Wösten (2001), Description of the unsaturated soil hydraulic database UNSODA version 2.0, *Journal of Hydrology, 251*(3), 151-162.

Nielsen, D., M. T. Van Genuchten, and J. Biggar (1986), Water flow and solute transport processes in the unsaturated zone, *Water Resour. Res., 22*(9), 89-108.

Njoku, E. G. and D. Entekhabi (1996), Passive microwave remote sensing of soil moisture, *Journal of hydrology, 184*(1), 101-129.

Philip, J. (1968), The theory of absorption in aggregated media, *Soil Research, 6*(1), 1-19.

Puhlmann, H., K. Von Wilpert, M. Lukes, and W. Dröge (2009), Multistep outflow experiments to derive a soil hydraulic database for forest soils, *Eur. J. Soil Sci., 60*(5), 792-806.

Rawls, W., Y. A. Pachepsky, J. Ritchie, T. Sobecki, and H. Bloodworth (2003), Effect of soil organic carbon on soil water retention, *Geoderma, 116*(1), 61-76.

Ross, P. and K. Smettem (2000), A simple treatment of physical nonequilibrium water flow in soils, *Soil Sci. Soc. Am. J., 64*(6), 1926-1930.

Schaap, M. G., F. J. Leij, and M. T. van Genuchten (2001), ROSETTA: a computer program for estimating soil hydraulic parameters with hierarchical pedotransfer functions, *Journal of hydrology, 251*(3), 163-176.

Schmugge, T. (1998), Applications of passive microwave observations of surface soil moisture, *Journal of Hydrology, 212*, 188-197.

Schultze, B., O. Ippisch, B. Huwe, and W. Durner (1997), Dynamic nonequilibrium during unsaturated water flow, Proceedings of the international workshop on characterization and measurement of the hydraulic properties of unsaturated porous media.

Schwarz, G. E. and R. Alexander (1995), Soils data for the conterminous United States derived from the NRCS State Soil Geographic (STATSGO) Database, *US Geological Survey Open-File Report*, 95-449.

Shin, Y., B. P. Mohanty, and A. V. Ines (2012), Soil hydraulic properties in one-dimensional layered soil profile using layer- specific soil moisture assimilation scheme, *Water Resour. Res., 48*(6).

Šimůnek, J., M. T. van Genuchten, and M. Šejna (2008), Development and applications of the HYDRUS and STANMOD software packages and related codes, *Vadose Zone Journal, 7*(2), 587-600.

Šimůnek, J. (2005), Models of water flow and solute transport in the unsaturated zone, *Encyclopedia of hydrological sciences*.

Šimůnek, J., N. J. Jarvis, M. T. Van Genuchten, and A. Gärdenäs (2003), Review and comparison of models for describing non-equilibrium and preferential flow and transport in the vadose zone, *Journal of Hydrology, 272*(1), 14-35.

Šimůnek, J. and M. T. van Genuchten (2008), Modeling nonequilibrium flow and transport processes using HYDRUS, *Vadose Zone Journal, 7*(2), 782-797.

Skopp, J. (1981), Comment on "micro-, meso-, and macroporosity of soil", *Soil Sci. Soc. Am. J., 45*(6), 1246-1246.

Thoma, S. G., D. P. Gallegos, and D. M. Smith (1992), Impact of fracture coatings on fracture/matrix flow interactions in unsaturated, porous media, *Water Resour. Res., 28*(5), 1357-1367.

Tuli, A., M. Denton, J. Hopmans, T. Harter, and J. MacIntyre (2001), Multi-step outflow experiment: From soil preparation to parameter estimation, *Land, Air and Water Resources Rep, 100037*.

US Natural Resources Conservation Service (1995), *Soil Survey Geographic (SSURGO) Data Base: Data use Information*, National Cartography and GIS Center.

Vachaud, G., A. Passerat de Silans, P. Balabanis, and M. Vauclin (1985), Temporal stability of spatially measured soil water probability density function, *Soil Sci. Soc. Am. J., 49*(4), 822-828.

Van Dam, J., J. Stricker, and P. Droogers (1994), Inverse method to determine soil hydraulic functions from multistep outflow experiments, *Soil Sci. Soc. Am. J., 58*(3), 647-652.

Van Genuchten, M. T. (1980), A closed-form equation for predicting the hydraulic conductivity of unsaturated soils, *Soil Sci. Soc. Am. J., 44*(5), 892-898.

Van Genuchten, M. T., F. Leij, and S. Yates (1991), *The RETC Code for Quantifying the Hydraulic Functions of Unsaturated Soils*, Robert S. Kerr Environmental Research Laboratory.

Van Genuchten, M. T. and P. Wierenga (1976), Mass transfer studies in sorbing porous media I. Analytical solutions, *Soil Sci. Soc. Am. J., 40*(4), 473-480.

Vogel, H., U. Weller, and O. Ippisch (2010), Non-equilibrium in soil hydraulic modelling, *Journal of hydrology, 393*(1), 20-28.

Wildenschild, D., J. Hopmans, and J. Simunek (2001), Flow rate dependence of soil hydraulic characteristics, *Soil Sci. Soc. Am. J., 65*(1), 35-48.

Yoo, C. (2002), A ground validation problem of remotely sensed soil moisture data, *Stochastic Environmental Research and Risk Assessment, 16*(3), 175-187.